STRUKTURA 2001

LECTURES - 18. 6.

Physics, materials, thin films

NEUTRON SCATTERING AT THE EDGE OF NEW MILLENIUM

Jiří Kulda

Institut Laue-Langevin, BP 156, 38042 Grenoble Cedex, France

The magnetic moment of neutron, the isotopic variation of its scattering length (contrast) as well as its kinetic energy comparable to that of thermal excitations make of neutrons an indispensable complement to X-rays in studies of microscopic properties of condensed matter. In the past decade the centers of scientific interest in neutron scattering have shifted from traditional fields involving magnetic, structural and dynamical properties of relatively simple crystals towards studies of more complicated objects – universality of phase transitions, physics of highly correlated electron systems, soft matter and biological objects. Many of these studies take advantage of the high penetrating power of neutrons, due to the absence of their electric charge, which facilitates experiments at extreme conditions, brought about by sophisticated sample environment equipments.

Since 1998 the Czech crystallographic community has full access to the world best neutron source - the recently refurbished high flux reactor of the Institut Laue-Langevin in Grenoble (France). At the same time the integration of Czech republic into the EC structures opens access to further, national size neutron laboratories offering support to external users and hosting unique, highly specialised equipments. While some of these smaller reactor sources are approaching their closing dates, new, more powerful facilities are coming to replace them. The new Munich reactor enters its commissioning stage and the funding aspects of projects for more distant future, AUSTRON and ESS (the Austrian and European spallation sources, respectively) are under discussion.

FIRST PRINCIPLES CALCULATIONS OF THE STRUCTURAL PROPERTIES OF SOLIDS

Martin Diviš

Charles University, Department of Electronic Structures, 12116 Prague 2, Czech Republic

The interactions of the electrons and ions in a solid are strong and long-range. Thus the task for the band theory is to find the ground states and possibly excitation spectra of strongly interacting many-body systems. Nonetheless, band theory, which uses a single-particle picture, is re-markably successful. This can be understood in terms of screening arguments. In a solid each electron is screened by other electrons, which avoid it. This screening renders the interaction between these "dressed electrons", or quasi-particles, much weaker than those between bare electrons. At least for some energy range the quasiparticles act as weakly interacting objects, for which band theory may be reasonable constructed. In band-structure calculations the problem of finding the many-body wavefunctions and eigenvalues for the interacting system is replaced by the solution of a series of one-particle Schrödinger-like equations, with an effective potential, which may be (i) dependent on the solutions, for example through the charge density, (ii) orbital- or energy-dependent and/or (iii) non-local. Moreover development of density-functional theory (DFT) has allowed replacement of the electronic wave-function with an equation in which the ground state electronic density n(**r**) or spin densities n↑(**r**), n↓(**r**) are the basic variables (Hohenberg and Kohn, 1964). Thus effective one-electron potential contains the following terms: (a) the Coulomb potential from the ions; (b) the average Coulomb (Hartree) potential due to other electrons; and (c) an electronic exchange-correlation contribution, which accounts for the tendency of each electron to be surrounded by an electron-depleted region. This effect is due to both the antisymmetry of the many-body wavefunction, which forbids close approaches between like-spin electrons, and the electrostatic repulsion between the electrons. The term (c) is difficult to calculate exactly and it is usually obtained by the local-density approximation (LDA) or by the local-spin-density approximation (LSDA), which assumes that the exchange-correlation energy density at a particular point **r** depends only on the local value of n(**r**) or n(**r**), n(**r**). This energy density can than be evaluated in the context of a uniform electron gas. The LDA (LSDA) has been extremely successful in accurately and reliably predicting the energetics of solids. This has led to its widespread use in predicting numerous properties of solids such as ground state structures and structural energy differences, magnetic ordering and values of the magnetic moments, elastic constants, phonon frequencies, high pressure equations of state, surface and interface geometry and alloy phase diagrams.

In this contribution we plan to demonstrate the practical application of the DFT method for the study of the nature of the 5f electrons in actinide intermetallic compounds. In contrast to the 4f-shell the 5f shell cannot be reasonably described using the perturbation theory of the localized and highly correlated atomic f-states. This is evident in many cases that 5f electrons contribute both to magnetism and bonding (conduction). Magnetism in actinide compounds is characterized by the presence of correlations associated with 5f-derived bands of a small bandwidth and energetically comparable spin-orbit interaction. Since the DFT is principally designed for description of the ground state and related properties (e.g. magnetic), we show, how the arguments for the 5f electron delocalization can be obtained from DFT calculations for isostructural *UTX* and *RTX* compounds ® = rare earth; *T* = transition metal; *X* = p-metal).

COHERENCE OF X-RAYS

Marian Čerňanský

Department of Metal Physics, Institute of Physics, Academy of Sciences of the Czech republic, Na Slovance 2, 182 21 Praha 8, Czech Republic

Fundamental notions describing the coherence of radiations are defined. A brief introduction into theory of partial coherence of optical fields is presented. Possible effects of the partial coherence are discussed, especially in the X-ray diffraction on crystals.

X-RAY DIFFRACTION AND X-RAY REFLECTIVITY APPLIED TO INVESTIGATION OF THIN FILMS

David Rafaja

Charles University, Faculty of Mathematics and Physics, Department of Electron Systems, Ke Karlovu 5, CZ-121 16 Prague

Scattering of X-rays is a commonly accepted technique for structure investigation of thin films and low-dimensional structures. The main reason is the small penetration depth of X-rays in solids that is typically less then some micrometers. Moreover, the penetration depth can be adjusted by changing the angle of incidence of the primary beam or changing the wavelength of the radiation. Typical features of thin films, which are usually studied by the X-ray scattering, are thickness of thin films, their interface quality and morphology, phase composition, residual stresses, crystallite size and preferred orientation of crystallites. With respect to the investigated characteristics of thin films, several experimental methods are employed that offer different insight into the real structure of thin films. The methods start with conventional X-ray diffraction (XRD), and include the glancing angle X-ray diffraction (GAXRD), X-ray reflectivity measurement (XRR) and grazing incidence X-ray diffraction (GIXRD). A concise information on the real structure of thin films can be obtained from the reciprocal space mapping.

Conventional XRD working in symmetrical mode is a typical representative of coplanar diffraction geometry. As for any coplanar geometry, the y component of the diffraction vector is equal to zero. In symmetrical mode, q_x is equal to zero as well. It means that only the length of diffraction vector can be varied; its direction is fixed. The coplanar symmetrical geometry is also used for the XRR measurements. The main difference between these techniques is in the scattering angles. Upon the reflectivity measurement, scans are performed at extremely low angles (typically $0 - 10° 2\theta$), whereas the conventional diffraction geometry covers the high-angle region (typically above $10° 2\theta$). Consequently, XRD yields mainly information about the real structure of thin films on atomic level. On the other hand, XRR is applied to get insight into the morphology of ultra-thin films, low dimensional structures and near-surface regions of materials.

In particular cases, e.g., measuring the lattice deformations due to the residual stress or studying the preferred orientation of crystallites, the direction of diffraction vector must be inclined from the normal direction. For thin films, GAXRD is a very popular technique, which offers the advantages of non-symmetrical diffraction geometry. Nevertheless, as GAXRD is a coplanar diffraction technique, it cannot access all parts of the reciprocal space. Its limitations are partly eliminated, when GIXRD is utilised. The lecture will discuss advantages and disadvantages of above diffraction techniques with special attention to the accessibility of reciprocal space, penetration depth and instrumental requirements. Applications of individual diffraction techniques will be illustrated by various examples of thin films and magnetic multilayers.

STRUCTURAL PROPERTIES OF SUPERLATTICES WITH LATERAL PERIODIC STRUCTURE

Zbyněk Šourek and Jiří Kub

Institute of Physics, Academy of Sciences of the Czech Republic, Na Slovance 2, 182 21 Praha, Czech Republic

Combining high resolution symmetrical and asymmetrical X-ray diffraction and X-ray reflectivity we have performed the structural investigation of series AlInAs/GaAs superlattices grown on GaAs (001) oriented substrates. The samples differing each other in the In content and in the number of bilayers have been grown in our institute by MOCVD technique on substrates with a miscut in the range from 0° to 3°. The combination of different X-ray scattering techniques [1,2] allows beside the non-destructive determination of the thickness and composition of layer sequences also the characterization of the morphology of interfaces. The system chosen enables us to follow the effects strong enough in both diffraction and reflection modes, in induces adequate strain in the diffraction experiments, Al sufficient contrast in the reflection mode.

The reciprocal space maps were measured in both modes, in the diffraction one in the quasisymmetrical reflections 004 and 002, always in the various azimuths of the scattering plane. The experiments were carried out by the double or triple crystal diffractometer Bede and Rigaku X-ray generator with rotating anode. CuK_α radiation was used. A perfect Ge single crystal was employed as monolithic monochromator, we utilized twice the 004 asymmetrical reflection for the diffraction mode and 111 for the reflection mode. Triple-crystal analyses were performed by inserting a four reflection Si (111) channel-cut crystal behind the sample to serve as an analyser.

The investigations revealed the well defined lateral periodicity of interfaces in the off cut samples. We suppose the interfaces are constituted by step-like (or may be better roof-like) objects. They were formed during growth through bunching of the miscut-induced monolayer steps

of the substrate surface. The elementary cell of this two dimensional superlattice structure is parallelogram. Its lattice vectors are neither parallel nor perpendicular to the surface. For miscut angle 3° e. g., they include about 5° and 167° with the surface. Parameters of this lattice seems to depend on the miscut angle only, they do not depend on the In concentration.

In the figure an example of the experimentally obtained reciprocal space map is given. From the distribution of patterns of the diffusion scattering the shape and parameters of the above mentioned elementary cell could be determined as well as the lateral periodicity of the bunch steps (from the distance of the perpendicular truncation rods).
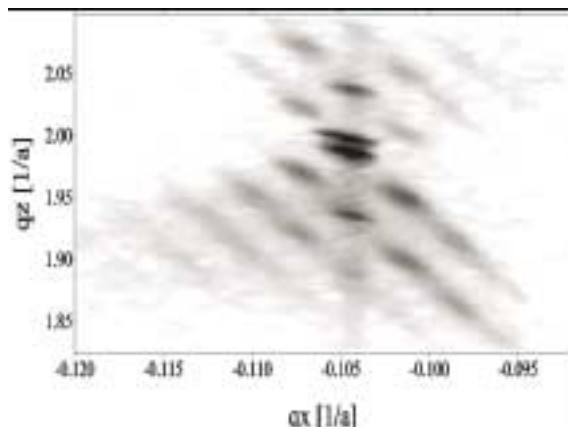
The reciprocal space map measured around the (002) reciprocal lattice point. $\{Al_{0.85}In_{0.15}As / GaAs\}$ superlattice grown on the 3° off cut GaAs 001 substrate.

The reciprocal space map measured around the (002) reciprocal lattice point. $\{Al_{0.85}In_{0.15}As / GaAs\}$ superlattice grown on the 3° off cut GaAs 001 substrate.

We compared the experimental results with theoretical calculations performed on the simple basis of the coherent scattering by point centres lying in the interface. It follows from them, that the shape of bunch steps depends strongly on the In concentration. In agreement with our experimental results it was approved that in the case of lower In concentration it is not possible to observe the patterns of the coherent diffusion scattering in the reflection mode and the information about the structure could be given by diffraction experiments only. For higher In concentration the misfit dislocations occur and relaxation take place. The maxima of the resonance diffuse scattering appear in the reflection experiments and the relaxation disables their observation in the diffraction mode.

1. V. Holý, U. Pietsch & T. Baumbach: *High-Resolution X-Ray Scattering from Thin Films and Multilayers.* Springer Verlag Berlin Heidelberg 1999

2. D. K. Bowen & B. T. Tanner: *High-Resolution X-Ray Diffractometry and Topography.* Taylor and Francis Lonon 1998

STRUCTURE AND SOME PROPERTIES OF FULLERITE

L. Sodomka[1], B. Knob[2], V. Šprta[2]

[1] *Department of clothing Textile faculty Technical university of Liberec, Hálkova 6, 46017 Liberec CR*

[2] *Research institute for chemistry (VUANCh) Revoluční 86, Ústí nad Labem, CR*
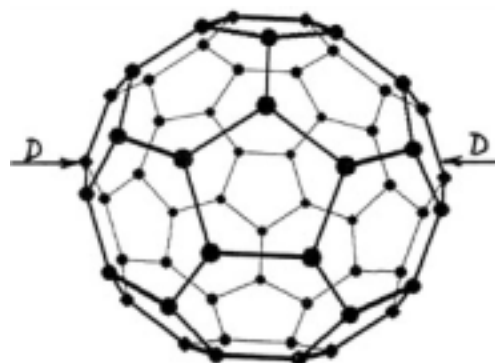
Figure 1. Fullerene C60

1. Introduction

The fullerites are belonging to the superstructure of the fullerenes, the closed carbon molecules. The most expanded form from the fullerenes is the fullerene C60 containing the 60 carbon atoms in the corner of the trancated twentyfaced object, s-icosahedron (Fig. 1). This molecule has been firstly described in the 1985 year by Curl, Kroto and Smalley [1]. Their discoverers have been awarded in the year 1996 through the Nobel price in chemistry. The fullerene molecule has been annonced in the year 1991 as a molecule of the year. Now it is getting the object of the contemporary research. It can be said, that the fullerenes and their aggregates wil be the object of the interest in the whole third milenium. Today there are existing many pappers about fullerenes and their derivatives in all modern world languages. The papers have been appeared as a results of the original work, over review articles also in
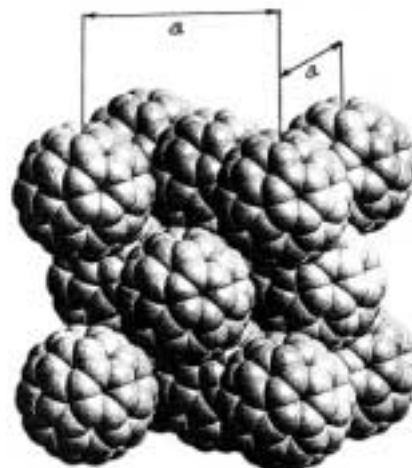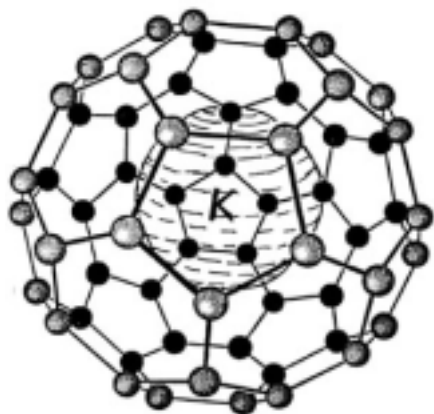

Figure 2. Fullerite

Figure 3. Fullerid with kalium atom in its inner

Czech [3, 4, 5, 6] to the popular scientific ones [7, 8] to the monographies [9, 10] to the proceedings from the conference [11].

The fullerene has been created as superstructure of the spherical molecules of the C60 fullerene. The fullerene molecules are creating the closed packed layer structure in it with the three layered periodicity of the type ... ABCAB-CABC... . It is necessary to note, that the two layered periodicity has not been observed to this time. The Three layered structure is creating the face centred cubic structure shown on the Fig. 2. The other layered superstructure as the hexagonal close packed structure has not been found as well as the superstructure of the higher periodicity. Because the diameter of the fullerene, sphere is approximately 0.7 nm and its volume is about the 0.34 cubic nanometers and the volume of the hydrogen atom is being is only 0.0001 cubic nanometers. It is following from the fact, that the fullerene molecule volume it can be placed about a thousand hydrogen atoms. To the fullerene volume there can be implanted also another atom as it is being shown in the Fig. 3 where there is an alkali metal atom in the fullerene innner. This structure has been called the fullerid. Through the modification of the fullerene there is a possibility of preparing of the all known properties of the solids. Therefore there is so high interest on the research of all modifications of the fullerenes. In this contribution, some structure parameters as well as properties of the fullerite have been studied.

2. X-ray spectral analysis of the fullerite

Since the fullerene molecule can be found in the fullerite structure, which is a solid (see Fig. 2), it seems quite natural to measure for example diameter and other characteristics of fullerenes on the fullerites. For the estimation of the physical properties of fullerites the first step is to measure chemical analysis of the fullerite probes delivered from the Hoecht as a coarse-grained powder. The probes contained 99.78 wt% of carbon and the 0.22 w% of other elements. To the identification of the other elements the phase analysis was made by the X-ray quantitative analysis which shown the following quantity of the elements in the fullerite: S - 0.163 wt%, Ba - 0.081wt%, Ar - 0.0275 wt%, Os - 0.0020 wt%, Fe - 0.0016 wt%, Zn - 0.0015 wt%. The

rest of the elements are belonging to the light elements to the element 10, which cannot be detected through the X-ray spectral analysis. The measurements have been made on Philips PW1404 spectrometer working with rhodium anode at the voltage 80kV using the germanium crystal ad the lithium fluorid one as monochromator elements using the Bragg reflexion (111) for Ge and (220) on LiF. The distribution of admixture atoms could not be determined with such a technique.

3. X-ray diffraction analysis of fullerite

To the determination of structure parameters the X–ray diffraction technique has been used. The diffractometer equipped with the copper X-ray tube with monochromator and Soller screen and wavelength 0.154 nm (CuKα) have been used. The diffraction curves are being shown on the Fig. 4 and 5. On Fig. 5, the two diffraction curves are being represented. They are corresponding to two probes, the original and milled ones. The diffration curves of the milled fullerite are shifted to the smaller Bragg angles, i.e. to the longer interplanar spacing d. The diffractograms on the Fig. 4, 5 have been indexed after [12], from single reflexions the interface distances calculated and the lattice parameters for each diffraction line determined. The order
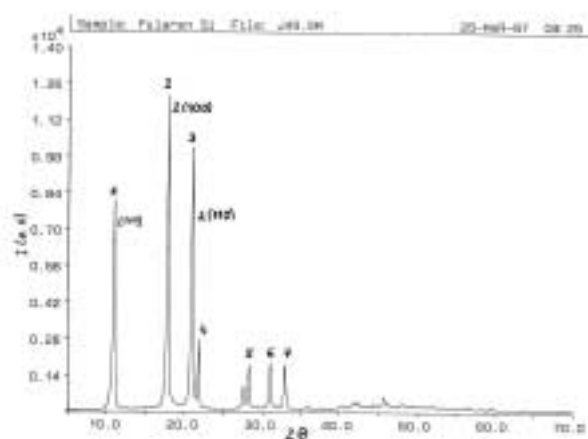

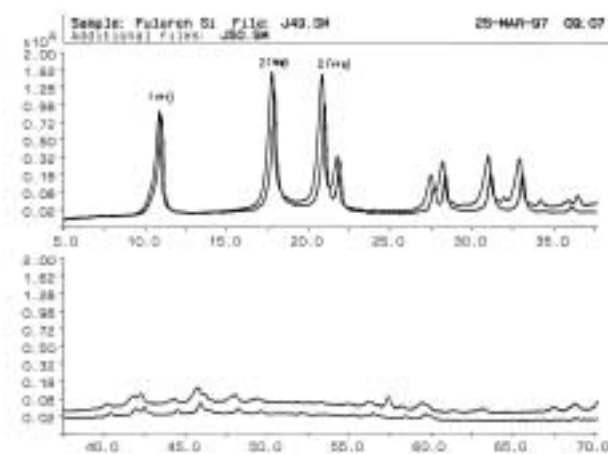**Figure 4.** Diffractograms of milled fullerite

Figure 5. Diffractograms of the original and milled fullerite

of the lattice parameters has been labelled in the accordance with the order of the diffraction lines. The value of the single a_i parameters are being as follows: $a_1 = 1.64$, $a_2 = 1$, $a_3 = 1.316$, $a_4 = 1.16$, $a_5 = 1,07$, $a_6 = 1$, $a_7 = 1.12$, $a_8 = 1,22$ nm. From the theoretical calculations made in [10] p.63, the C60 fullerene diameter has been calculated and obtained the value D = 0,71nm. The lower measured value can be interpreted the attraction of the elastic fullerene spheres and their compressing. The different values of the fullerite lattice parameters can be explained by the geometric anisotropic sphere deformation.

4. Some physical properties of fullerite

In the reference [10] some different physical properties of the fullerite have been demonstrated as the electrical, photoelectrical conductance and luminescence. These properties have been found also in our samples of the fullerite. The measurements of the fullerite resistivity have shown the value of the order $10^{14}\Omega$.m and it is nearly nonconductive. The photoconductivity stimulated through the nitrogene laser and crypton discharche tube as ell as the mechanoluminescence [13] has not been observed. Because the introduced measured properties are being structure sensitive and in [10] the compositon and admixtures have not been introduced, the different results are not being astonishing.

5. Evaluation and conclusion

The solution of some structure parameters of the fullerite have shown that our fullerite had the cubic face centred lattice with the lattice points created through the C60 fullerene balls. Through the acting of the attractive forces between the balls analogical to the metal bonding and elasticity of the fullerene balls is the fulletite lattice in certain direction with the smaller ball density being deformed and the experimentally determined ball diameter 0.66nm is being smaller than theoretically one. X-ray spectral analysis has shown the presence of the admixture of the sulphur in 0.163 w% and barium in 0.0810 w% which the structural sensitive studied physical properties have not been influenced through.

The paper is being dedicated to the 20th not ending she s life birthday of the daughter Magdalena Sodomková..

References

1. Kroto, H.V. et al.: *Nature* **318** (1985) 162.

2. Sodomka, L.: Nobelova cena za objev fulerenu. *MFI* **7** (1997) 63. Sodomka, L., Sodomková, M.: Nobelovy ceny za fyziku. SetOut Praha 1997.

3. Matyáš, M.: Fullereny a fullerity. *PMFA* (1992) 288.

4. Jech, Č.: Fullerenová allotropní forma uhlíku. *Čs. Čas. Fyz.* **42** (1992) 337.

5. Kraetchmer, W. AnH- Magazin NO.62 Dezember 1993, p.11[6].

6. Sodomka, L., Sodomka, J.: Historie objevu fullerenu a jejich derivátů. *MFI* (1998) 216.

7. Sodomka, L., Sodomka, J.: Diamanty a ježci vkleci. *T97* **40** (1997) 22.

8. Valenta , J. Nejkulatěší molekula. *Vesmír* **76** (1997) 65.

9. Koruga, G., et al.: Fulllerene C60. North Holland Amsterodam 1963.

10. Dresselhaus, M.S., et al.: Science of fullerenes and carbon nanotubes. Academic Press, New York 1996.

11. Andreoni, W.: The chemical physics of fullerenes 19 (and 5) years later. NATO ASI series E:Applied Science , Kluwer academic Publisher, Dornrecht 1996.

12. Sodomka,L.: Rentgenová difraktografie pevných látek. SNTL Praha 1960.

13. Sodomka,L.:Mechanoluminiscence a její použití. Academia Praha 1985

LECTURES - 19. 6.

Teaching

USE OF INTERNET FOR TEACHING CRYSTALLOGRAPHY

Radomír Kužel

Faculty of Mathematics and Physics, Charles University, 121 16 Praha 2, Ke Karlovu 5

It is only a question of time when the Internet will be dominating communication tool also for teaching.

David Kříž, a student of Faculty of Mathematics and Physics, started the work on WWW pages for teaching crystallography last year. The pages are based on the text book written by V. Valvoda, M. Polcarová and P. Lukáč: Základy strukturní analýzy (Karolinum, Praha 1992). However, the original form is being gradually improved by new figures, animations and exercises. The working version can be found at http://www.xray.cz/krystalografie and all suggestions and tips for improvement are highly appreciated. At present time, a part of crystallography is already quite well developed while the part of structure analysis should still be significantly improved.

Last year, different on-line courses on crystallography and X-ray diffraction appeared. They offer different certificates and, of course, they are not free of charge. In general, useful educational resources can be found on the IUCr web pages http://www.iucr.ac.uk under CWW (Crystallography World Wide) in section *Education Online* http://www.iucr.ac.uk/cww-top/edu.index.html.

Unfortunately, many of the pages are nothing more than books transformed into HTML form.

IUCr teaching pamphlets can be found at http://www.iucr.ac.uk/iucr-top/comm/cteach/pamhlets.html.

Some worthwhile crystallographic Web sites sites will be shown in the lecture.

LECTURES - 20. 6.

Structural Databases

CAMBRIDGE STRUCTURAL DATABASE - CSD

The Cambridge Structural Database (CSD) contains crystal structure information for over 230,000 organic and metal organic compounds. All of these crystal structures have been analysed using X-ray or neutron diffraction techniques.

For each crystallographic entry in the CSD there are three distinct types of information stored. These are conveniently categorised in terms of their "dimensionality".

1D Information. These data fields incorporate all of the bibliographic material for the particular entry and summarise the structural and experimental information for the crystal structure. The text and numerical information includes the authors' names and the full journal reference, as well as the crystallographic cell dimensions and space group.

2D Information. A conventional chemical diagram of the molecule is stored in this information field. This is encoded as a chemical connection table comprising atom and bond properties. Atom properties include element symbol, number of connected non-hydrogen atoms, number of connected hydrogen atoms, and the net charge. Seven different bond types can be specified in bond properties.

3D Information. A 3D representation of the molecule can be generated from the information stored in this field. This data includes the atomic coordinates, the space group symmetry, the covalent radii and the crystallographic connectivity established by using those radii. The 3D representation is matched with the 2D chemical structure.

(From http://www.ccdc.cam.ac.uk/)

Contribution on CSD will be given by S.J. Maginn

THE PROTEIN DATA BANK - AN INSIDER'S PERSPECTIVE

The Research Collaboratory for Structural Bioinformatics

Rutgers University, Piscataway, NJ; San Diego Supercomputer Center, University of California, San Diego, La Jolla, CA; National Institute of Standards and Technology, Gaithersburg, MD

The Protein Data Bank (PDB; http://www.pdb.org/) is the international repository for the processing and distribution of three-dimensional structural data. The PDB has developed several integrated tools for the deposition of structures and query of the archive and provides many resources for understanding the structure of biological macromolecules.

The PDB AdIt, the AutoDep Input Tool (http://.rutgers.edu/adit/), is used by the community for the deposition and validation of data to be included in the PDB archive. To deposit a structure, the user uploads the relevant coordinate and experimental data files and then adds any additional information.

AdIt is also used internally by the PDB for data processing. Its architecture allows not only distributed depositions from depositors all over the world but also distributed annotation at several RCSB annotation stations. We are proud to announce that one of annotation stations has been set up in Prague in collaboration with the Czech and Slovak Crystallographic Association.

Several query and reporting interfaces have been developed to search across the PDB archive (http:// www.rcsb. org/pdb/). SearchLite provides simple keyword searches. SearchFields is a customizable query interface that offers more detailed searching. Search results can be examined by generating reports about individual or multiple structures.

These systems, as well as our plans for further extending the capabilities of the PDB, will be described. The PDB is managed by the Research Collaboratory for Structural Bioinformatics (RCSB). The vision of the RCSB (http://www.rcsb.org/) is to enable new science by providing accurate, consistent, and well annotated structure data via the application and development of modern information technology.

Contribution will be given by B. Schneider

THE INORGANIC CRYSTAL STRUCTURE DATABASE

The Inorganic Crystal Structure Database (ICSD) contains complete structural information for inorganic compounds, including compound name, molecular formula, crystal symmetry group, unit cell parameters, atomic coordinates, and temperature factors. Sources for ICSD are original journal articles. Bibliographic information, property information, and indexing terms are searchable.

ICSD includes information on all crystal structures which contains at least one of the non-metallic elements H, He, B, C, N, O, F, Ne, Si, P, S, Cl, Ar, As, Se, Br, Kr, Te, I, Xe, At and Rn which have no C-C and/or C-H bonds whose atomic coordinates are determined carbides and zeolites (also with organic host molecule).

Database is produced by FIZ Karlsruhe, Gmelin Institute, journals coverage since 1912, database is updated bi-annually. Last version contains 56 875 structures.

References

http://www.fiz-karlsruhe.de/stn/Databases/ icsd.html
User manual ICSD, 1995

Demonstration given by I. Císařová

POWDER DIFFRACTION FILE AND SUPPORTING SOFTWARE FROM ICDD

Latest release 2000 of the Powder Diffraction File™ (PDF-2) from International Centre for Diffraction Data (ICDD) contains patterns representing over 131,000 phases, including 2,500 new experimental patterns compiled through the ICDD®'s Grant-in-Aid program and literature searches, and 4,500 new calculated patterns from the ICSD. (ICSD is the Inorganic Crystal Structure Database maintained by Fachsinformationzentrum (FIZ) in Karlsruhe.)

The Powder Diffraction File™ (PDF-2) is the world's largest and most complete collection of X-ray powder diffraction patterns. Each pattern includes a table of interplanar (d) spacings, relative intensities (Int), and Miller indices, as well as additional helpful information such as chemical formula, compound name, mineral name, structural formula, crystal system, physical data, experimental parameters, and references. In addition, the ICDD® editors have assigned each experimental pattern a quality mark, which indicates their estimate of reliability.

PCPDFWIN is Windows® based retrieval/display software for accessing records from the ICDD Powder Diffraction Database, known as the PDF-2. Complex searches of the PDF-2 may be carried out by combining Boolean operators and chemical and physical properties, elemental and crystallographic information, compound names, subfiles, literature references, and/or strong lines.

PCSIWIN is a new computer program designed to provide the functionality of the Hanawalt and Fink Search Manuals. Data input accommodates d/I pairs for up to 40 lines. If the wavelength is specified 2theta/I pairs can be used. The user can customize the size of the database by using filters for subfiles, chemistry, and number of elements. An automatic history function keeps track of results from previous sessions.

The PC SEARCH INDEX program is designed to fulfill the role of an "electronic search manual". It is not designed to be a "search/match" program in the generally accepted definition of this term. A search/match program is intended to provide possible solutions to a submitted set of experimental powder data, where the operator's role is restricted to the setting up of a set of search parameters, followed by which, the computer will do its best to come up with a set of matches for the lines (and perhaps also the intensities) of the experimental data set. A search manual is designed as a tool to assist the user in personally allocating lines in the experimental pattern to single phases of the user's choice. Thus a true "search/match" program gives a complete solution in one pass. Search manuals (and, therefore, PCSIWIN) give answers sequentially, with the operator making decisions after each pass. Several classical systematic approaches have been developed over the years, of which the Hanawalt and Fink methods are the best known.

References

http://www.icdd.com

Demonstration: R. Kužel

Minerals

STRUCTURE AND PROPERTIES OF SiC POLYTYPES

Slavomil Ďurovič

Institute of Inorganic Chemistry, Slovak Academy of Sciences, SK-842 36 Bratislava, Slovakia

A two-dimensionally periodic layer with layer-group symmetry $P(6/m)mm$ is the natural basic building unit for all structures based on the close packing of equal spheres [1]. The limits for the stacking of such layers are given by the fact that the spheres of the next layer can occupy only one of the two, translationally non-equivalent voids, so that the position of the spheres of any layer can be only A, B or C. Based on this principle, an infinite number of periodic but also non-periodic (in the stacking direction) structures is possible; the best known - also as *standard* or *MDO polytypes* - are the cubic (f.c.c.) and hexagonal (h.c.p.) ones. The individual structures are known as *polytypes* and belong to one *family*. Typical for close-packed structures are structures of some metals as *e.g.* Al, Cu, Au, Ag (f.c.c.), Mg, Zr (h.c.p.) or Co (both arrangements).

A closer look reveals that the symmetry $P(6/m)mm$ holds only for individual layers taken separately. Any stack of layers has necessarily a reduced symmetry. Thus some operations of the layer group cannot enter a space group of the resulting structure (if periodic) and remain *partial*. As shown by Dornberger-Schiff [2], see also [3], such partial operations are in fact responsible for the ambiguity in the stacking - *i.e.* for polytypism. The set of all total and partial operations in a polytypic structure constitute a *groupoid.* The value Z giving the number of the positions of a layer which, together with the preceding layer form geometrically equivalent pairs is given by the ratio N/F, where N is the order of the subgroup of those operations of the layer group which do not convert the layer upside down and F is the layer group of the pair of adjacent layers.

In any close packing of equal spheres, there are tetrahedral and octahedral cavities which can be filled by smaller atoms yielding thus a wide variety of structures as SiC, ZnS, AgI, but also CdI_2, PbI_2, SnS_2, $NbSe_2$, $Al(OH)_3$, $Mg(OH)_2$, *etc.*

The structures of the polytypes of silicon carbide (SiC) can be derived from the close packing of Si atoms if a half of all tetrahedral cavities are occupied by C atoms: the symmetry of individual Si-C double layers is, relative to $P(6/m)mm$, reduced to $P(6)mm$. All polytypes can be unambiguously described by *descriptive symbols* (ABC sequences, Hägg, Zhdanov symbols) or by *indicative* Ramsdell symbols.

The two standard polytypes, cubic and hexagonal, contain only one kind of layer triples each: ABC and ABA, respectively. All other polytypes contain both kinds of layer triples in various proportions. The percentage α of the ABA triples is sometimes, but incorrectly, called *index of hexagonality.* This term may be used as laboratory jargon only, never in serious publications.

Studies on single crystals of various SiC polytypes carried out at the former Leningrad Electrotechnical Institute [4] showed that not only the lattice geometry but also the chemical composition, thermodynamical and electrical properties vary almost linearly with the index α. This indicates the possibility of tuning-up the properties in a purely structural way - without admixtures. Recently also structure refinements of two SiC polytypes [5] revealed significant differences in the structure of individual layers depending on whether they are in an ABC or in an ABA environment.

1.   D. Pandey & P. Krishna *in* International Tables for Crystallography, Vol.C (Eds. A.J.C. Wilson and E.Prince). Dordrecht/Boston/London 1999, pp.744-752. Kluwer Academic Publishers.

2.   K. Dornberger-Schiff, *Abh. Dtsch. Akad. Wiss.* Berlin, Kl. f. Chem. **3** (1962).

3.   S. Ďurovič *in* International Tables for Crystallography, Vol.C (Eds. A.J.C. Wilson and E.Prince). Dordrecht/Boston/London 1999, pp.752-765. Kluwer Academic Publishers.

4.   Yu.M. Tairov & V.F. Tsvetkov *in* Crystal Growth and Characterization of Polytype Structures, (Ed. P. Krishna). Oxford/New York/Toronto/Sydney/Paris/Frankfurt pp. 111-161. Pergamon Press.

5.   A. Bauer, Ph. Reischauer, J. Kräusslich, N. Schell, W. Matz & K. Goetz, *Acta Cryst.* A**57** (2001) 60-67.

SYNTHETIC Cs FERRI-ANNITE - A POTENTIAL NUCLEAR WASTE DISPOSAL PHASE: ITS CRYSTAL STRUCTURE AT ELEVATED TEMPERATURE AND PRESSURE

Milan Rieder

Institute of Geochemistry, Mineralogy and Mineral Resources Charles University, 12843 Praha 2, Czech Republic

The generally high mobility of alkalies and the large ionic radius of Cs^+ are the key obstacles in efforts to immobilize radioactive isotopes ^{135}Cs and ^{137}Cs, which belong among the most troublesome products of nuclear fission. There are very few natural phases that can accommodate cesium, but some micas can. Therefore, we synthesized micas with Cs as the sole interlayer cation and studied them further. For safety, we used non-radioactive cesium.

Cs micas were grown from oxide mixes of appropriate stoichiometry under standard hydrothermal conditions (100 MPa hydrostatic pressure, T up to 610°C) [1]. Nanpingite, the Cs analog of muscovite $(CsAl_2AlSi_3O_{10}(OH)_2)$, could not be grown in good yields, but the Cs analog of annite $(CsFe^{2+}_3AlSi_3O_{10}(OH)_2)$ could. Due to an experimental failure (a burst tube), aluminum-free Cs tetra-ferri-annite was grown in excellent crystals. Subsequently, it was synthesized in a programmed fashion and

studied further. This talk will concentrate on the two annite-related latter micas.

The crystal structure of the Cs tetra-ferri-annite was refined from single-crystal data (ambient conditions [2]), but the structure of the Cs analog of annite did not yield suitable crystals and had to be refined by the Rietveld technique [1]. Single-crystal intensities from Cs tetra-ferri-annite were also collected in high-temperature and high-pressure devices [3].

The crystal structures of both cesium annites have a number of common features. First, Cs^+ is a very large cation and Fe^{3+} is larger than Al. Consequently, the unit cells are large and the structures are close to the textbook models; in fact, Cs tetra-ferri-annite appears to be among the geometrically most ideal mica structures refined to date. Second, high-temperature and high-pressure experiments show a differentiated expansion and compressibility of individual sheets in the structure and indicate a pattern of geometrical distortions of coordination polyhedra. Third, from a summary of related research done by ourselves and others it follows that different univalent interlayer cations have different bulk moduli.

Important for nuclear technology is the fact that trioctahedral cesium micas grow easily and with good crystallinity, and their crystal structures appear to accommodate Cs^+ without strain. They are stable over a wide range of p, T conditions, and the leachability of cesium from them is low (lower than for pollucite) [4]. These micas thus could be used as nuclear waste disposal phases for ^{135}Cs and ^{137}Cs.

New crystallographic data on Cs micas obtained expand the existing general knowledge about the crystal structure of the micas. The different compressibilities of different univalent interlayer cations have important implications for substitutions in micas under high-grade metamorphism and will have to be reflected in geothermometric and geobarometric algorithms.

In the talk will be presented photographic documentation as well as tabelations and graphs documenting the main conclusions.

References

1.   M. Drábek, M. Rieder, C. Viti, Z. Weiss & J. Fr, *Canad. Mineral.* **36** (1998) 755-761.

2.   M. Mellini, Z. Weiss, M. Rieder & M. Drábek, *Eur. J. Mineral.* **8** (1996) 1265 - 1271.

3.   P.Comodi, P.F. Zanazzi, Z. Weiss, M. Rieder & M. Drábek, *Amer. Mineral.* **84** (1999) 325-332.

4.   Z. Klika et al., *Appl. Geoch.* (submitted)

X-RAY DIFFRACTION STUDY OF MINERALS IN Fe$_3$P-Ni$_3$P SOLID-SOLUTION

R. Skála[1], I. Císařová[2] and M. Drábek[1]

[1]*Czech Geological Survey, Geologická 6, CZ-15200 Praha 5, Czech Republic, correspondence author's e-mail address: skala@cgu.cz*
[2]*Dept. of Inorganic Chemistry, Charles University, Hlavova 2030, CZ-12843 Praha 2, Czech Republic*

Phosphides of Fe$_3$P-Ni$_3$P solid solution are quite common constituents in many iron-rich differentiated meteorites (with bulk phosphorus content higher than 0.06 wt. %) [1], they are found also as an accessory phase in other groups of silicate-dominating meteorites [2], lunar rocks [3] and they have been encountered in burning coal seams in France (Commentry) [4] and on the bottom of the Red Sea [5] in terrestrial conditions, too. In this solid solution, two minerals are defined – schreibersite [6] and nickelphosphide [7]. Also, the variety name rhabdite is used to identify tiny crystals of schreibersite/ nickelphosphide with prismatic habit [8].

Earlier studies of phase relations within the ternary Fe–Ni–P system [9] revealed complete solid solution between Fe$_3$P and Ni$_3$P with no miscibility gaps. Moreover, Shunk [10] mentioned Fe$_3$P as being isotypic with Ni$_3$P.

A crystal structure motif of (Fe,Ni)$_3$P phases (tetragonal, *I*, *Z* = 8, all elements in 8*g* sites, three crystallographically non-equivalent sites occupied by metals) was described on the compound Ni$_3$P [11]. Later, the crystal structure of meteoritic schreibersite of Fe$_2$NiP composition was solved and refined [12] from data collected on the rhabdite crystal from the Tocopilla (Chile) iron meteorite. Both of the latter refinements differ in site occupancies for nickel and iron, nevertheless, both indicate non-equal Fe/Ni partitioning within the schreibersite crystal structure. The fact of non-equal site occupancies in this type of compounds is supported also by recent refinements of neutron powder data for compounds (Fe$_{1-x}$Co$_x$)$_3$P [13].

Experimental:

Single-crystal data of schreibersites recovered mechanically and/or chemically from iron meteorites were acquired using Nonius KappaCCD diffractometer employing Mo radiation. The meteoritic irons sampled were Carlton, Odessa, Sao Juliao de Moreira, Sikhote Alin, and Toluca. Crystal structure data were refined by program JANA2000 [14].

For powder diffraction study, the members of Fe$_3$P-Ni$_3$P solid solution with selected chemical composition have been synthesized in evacuated, sealed silica tubes. Runs were repeatedly reground under acetone and re-heated at given temperature. Experimental runs were quenched by dropping the charges in ice water. Phosphides were synthesized from mixes of iron, nickel and red amorphous phosphorus. The reaction products were examined by reflected light microscopy and electron probe microanalysis. Some runs are accompanied by very small quantities of iron phosphates.

Powder diffraction data of synthesized materials have been collected using Philips X'Pert MPD (reflection geometry, Cu*K*α radiation) and/or STOE STADI P (transmission geometry, Co*K*α1 radiation) diffractometers. To yield unit-cell dimensions from powder data we have applied two distinct approaches. We used whole-pattern profile fitting (WPPF) and individual peak profile fitting (IPPF) followed by an indexing of reflections based on calculated intensity patterns from structure data. The programs used were FullProf2.k [15], XFit [16] and that of Burnham [17].

Results:

Collection of reasonable data from natural materials finally appeared to be more complicated than expected. Schreibersite grains or rhabdite prisms displayed quite often various defects, mosaicism or they have been found to be partially or completely decomposed after chemical leaching used to obtain the material from solid pieces of meteoritic iron. Eventually, we were able to collect reasonable data set for samples coming from meteorites Carlton, Odessa and Siktote Alin. Our data confirm non-equal partitioning of Fe and Ni over crystallographically non-equivalent sites within the crystal structure and we also find that the absolute structure of all single crystals of (Fe$_{1-x}$Ni$_x$)$_3$P phases from meteorites differs from that reported traditionally.

Unit-cell dimensions yielded by both adopted methods (i.e. WPPF and IPPF) differ slightly but the general compositionally-dependent trend remains retained for both data sets. Parameters vary in relatively broad ranges with chemistry – the difference between unit cell dimensions of end-members reaches up to 1.7 rel. %. Generally, it holds that the higher content of Fe$_3$P end-member the higher length of both unit-cell parameters is encountered. Variation of unit-cell dimensions with the iron content is plotted in Fig. 1.
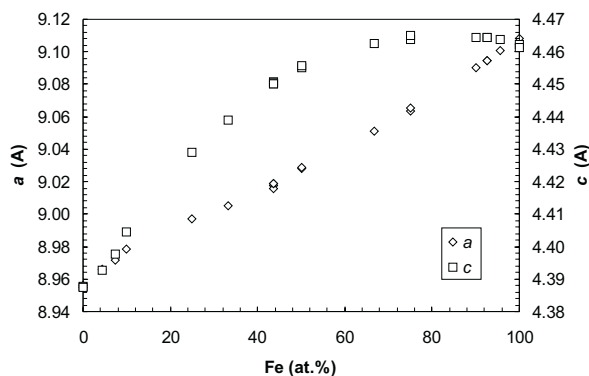

Figure 1. Variation of unit-cell dimensions of members of (Fe$_{1-x}$Ni$_x$)$_3$P solid solution. The higher iron content the higher length of unit-cell dimensions.

Conclusions:

Our refinements from single-crystal data unambiguously supports the previous observations [12,13] indicating non-equal distribution of metallic atoms over individual sites within the crystal structure of schreibersite-nickelphosphide minerals.

Unit-cell dimensions clearly vary with varying chemical composition of the synthesized phosphides studied. Variation is more or less linear for parameter a whereas for parameter c the trend is non-linear and asymmetric with a little change close to Fe_3P end member (Fig. 1). The solid solution Fe_3P-Ni_3P departs from modified Vegard's rule taking into account a volume aditivity in solid solutions [18] – volumes of both end-members are considerably lower than expected from other volume data in the solid solution. Instead of linear variation the volume seems to depend on the chemical composition in a more complicated way. Such departure from ideal behavior has already been observed and discussed for common silicate and oxide binary solid solutions in [19]. Perhaps, the trend observed for variation of unit-cell volume with chemical composition might be explained by the concept of non-equivalent site (NS) volume behavior [19] reflecting the fact that there are three crystallographically non-equivalent structure sites in the structure of schreibersites. These sites are generally of various geometries and therefore a kind of preferential occupation by either iron or nickel may produce the observed unit-cell variation trend.

The preference in occupation of particular sites within the structure by certain type of atoms refined from single crystal data and inferred from powder data however could not be explained solely by geometrical factors – atomic radii of involved metals are extremely close each other so there is no reason why e.g. nickel occupies preferentially one site and iron dominates in other two ones. Instead, it is quite possible that thermodynamics and kinetics play an important role in non-equal partitioning of metals over crystallographically non-equivalent sites. This, in turn, could provide, when properly calibrated, a useful independent tool for estimates of pT-histories of iron meteorites containing schreibersite-series minerals from crystal structure data and hence of their parent bodies.

References:

1. V.F. Buchwald: Handbook of Iron Meteorites. Vol. 1: Iron Meteorites in General. Berkeley 1975. Univ. California Press.

2. A.J. Brearley & R.H. Jones, *Reviews in Mineralogy*, 36 (1998) 3-1 – 3-398, D.W. Mittlefehldt *et al.*, *Reviews in Mineralogy*, 36 (1998) 4-1 – 4-195.

3. J.J. Papike, *Reviews in Mineralogy*, 36 (1998) 5-1 – 5-234.

4. E. Mallard, *Bull. Soc. Min.* 4 (1881) 230; cited in E.S. Dana: The System of Mineralogy of James Dwight Dana, 6th Ed., page 31. New York 1892. John Wiley & Sons.

5. Yu.S. Borodaev *et al. Zapiski Vsesoyuz. Min. Obshch.*, 111 (1982) 682–687.

6. W.K. von Haidinger, *Annalen der Physik*, 72 (1847) 580–582.

7. S.N. Britvin *et al.*, *Zapiski Vseros. Min. Obshch.*, 128 (1999) 64–72.

8. G. Rose *Abh. Akad. Wissen.*, 1863 (1864) 23–161.

9. R. Vogel & H. Baur *Archiv für das Eisenhüttenwesen*, 5 (1931) 269–278 and A.S. Doan & J.I. Goldstein *Metall. Transactions*, 1 (1970) 1759–1767.

10. F.A. Shunk: Constitution of binary alloys. New York 1969. McGraw–Hill.

11. B. Aronsson, *Acta Chem. Scand.*, 9 (1955) 137–140; S. Rundquist *et al.*, *Acta Chem. Scand.*, 16 (1962) 242–243 and E. Larsson, *Arkiv för Kemi*, 23 (1965) 335–365.

12. F.D. Doenitz, *Naturwissen.*, 55 (1968) 387 and F.D. Doenitz, *Zeit. Kristall.*, 131 (1970) 222–236.

13. H.-p. Liu *et al.*, *J. Magn. Magn. Mater.*, 189 (1998) 69–82.

14. M. Dušek & V. Petříček, *Mater. Struct.*, **5** (1998) 277 and M. Dušek & V. Petříček (2001): JANA2000 – a computer program, Inst. Phys., Czech Acad. Sci., Prague, Czech Republic.

15. J. Rodríguez-Carvajal, *Physica B*, **192** (1993) 55-69 and J. Rodríguez-Carvajal (2001): FullProf.2k. – a computer program.

16. A. A. Coelho & R.W. Cheary (1996): X-ray Line Profile Fitting Program, XFIT.

17. C.W. Burnham, *Carnegie Inst. Yb.*, 61 (1962) 132–135.

18. E-an Zen, *Amer. Mineral.*, 41 (1956) 523–524.

19. R.C. Newton & B.J. Wood, *Amer. Mineral.*, 65 (1980) 733–745.

LOW-TEMPERATURE Ni-RICH LÖLLINGITE FROM HÁJE, PŘÍBRAM, CZECH REPUBLIC. RIETVELD CRYSTAL STRUCTURE REFINEMENT

P. Ondruš, I. Vavřín, R. Skála, and F. Veselovský

Czech Geological Survey, Klárov 131/3, CZ 118 23 Prague 1, Czech Republic.

Ni-rich löllingite is described from silver mineralization of the complex uranium-polymetallic deposit of Háje ore nodal point, 4 km SE of Příbram. A new paragenetic type – called thereafter "löllingite" – is described in the paper. Major minerals of this paragenesis are Ni-löllingite, roscoelite, calcite (of stage K5), pyrrhotite, galena, silver, and acanthite. Ni-löllingite forms radial spherulitic huddles of trillings composed of thin lenticular- or spindle-shaped crystals about 2 mm long and 100 μm thick. Trillings on (101) yield very nice well-developed stellate shapes specimens in cross-sections. The color is silver-metallic. The elongation of observed Ni-löllingite crystals is along axis b. Recalculation of average of 8 chemical analyses on the

basis of 3 atoms pfu gives the empirical formula $(Fe_{0.61}Ni_{0.36}Co_{0.04})_{\Sigma=1.01} (As_{1.94}S_{0.01}Sb_{0.03})_{\Sigma=1.98}$. Unit cell dimensions and densities from the Rietveld crystal structure refinement (assuming orthorhombic s.g. Pnnm and Z = 2) are a = 5.243(1), b = 5.978(1), c = 2.9783(6) Å, D_x = 7.371(3) g/cm^3 for Ni-löllingite from Háje and a = 5.2684(2), b = 5.9631(3), c = 2.9007(1) Å, D_x = 7.496(1) g/cm^3 for löllingite from Dolní Bory. Correlation between individual unit cell parameters and molar ratio R = Fe/(Fe+Ni) computed from data for members of $FeAs_2$ - $NiAs_2$ series gives regression equations: a [Å] = -0.5319·R^2 + 1.0795·R + 4.7560, b [Å] = -0.1971·R^2 + 0.3899·R + 5.7937, c [Å] = 0.5416·R^2 - 1.2114·R + 3.5476. The parameter R can be satisfactorily estimated from equation R = 1.01475- √(9.9712 – 1.8800·a). In the present work crystal structures of Ni-löllingite from Háje and löllingite from Dolní Bory are refined. Also, low-temperature conditions under which studied Ni-löllingite trillings formed and their morphology are discussed in detail.

Powder Diffraction, Materials

POROVNANIE APROXIMAČNÝCH A FOURIEROVSKÝCH DEKONVOLUČ- NÝCH METÓD PRI ANALÝZE RTG DIFRAKČNÝCH PROFILOV

Stanislav Jurečka

Katedra fyziky, Vojenská akadémia, Liptovský. Mikuláš

Pri analýze experimentálneho difrakčného profilu predpokladáme, že experimentálny profil je konvolúciou fyzikálneho profilu a prístrojovej funkcie. Pod fyzikálnym profilom rozumieme difrakčný profil rozšírený len v dôsledku vlastností difraktujúceho objektu. Tvar prístrojovej funkcie je určený vlastnosžami dopadajúceho žiarenia a geometrickým usporiadaním experimentu. Pri analýze fyzikálneho profilu difrakčnej línie sa používa viacero dekonvolučných metód. Fourierovské dekonvolučné metódy využívajú skutočnosž, že fourierov obraz konvolúcie funkcií je súčinom fourierovských obrazov jednotlivých funkcií. Obraz fyzikálneho profilu difrakčnej línie je možné skonštruovaž pomocou obrazov experimentálneho difrakčného profilu a štandardu. Spätnou fourierovou transformáciou je potom možné určiž fyzikálny difrakčný profil. Podrobne sa analyzujú vlastnosti fourierovej transformácie a podmieky jej využitia pri dekonvolúcii fyzikálneho profilu (vzorkovanie, aliasing, filtrácie vysokofrekvenčnej zložky). Pri praktickej aplikácii fourierovských dekonvolučných metód sa využíva grafické interaktívne rozhranie, ktoré umožňuje bezprostredné vyhodnotenie jednotlivých krokov dekonvolučnej metódy.

Aproximatívne dekonvolučné metódy používajú pri určovaní parametrov fyzikálneho difrakčného profilu zjednodušený model, v ktorom sa analyzujú uhlové závislosti vybraných charakteristík experimentálneho profilu a profilu štandardu. Funkcie, popisujúce tieto uhlové závislosti, určujú požadované charakteristiky profilov pre určitú konkrétnu voľbu funkcií, aproximujúcich difrakčné profily. V tejto práci je pre porovnanie s fourierovskými metódami použitá aproximácia difrakčných profilov modifikovanou funkciou Pearson VII. Výstupom týchto metód je sada charakteristík fyzikálneho profilu difrakčnej línie, ktoré sa ďalej používajú pri analýze mikrodeformácií a veľkosti oblasti koherentného rozptylu.

Na základe porovnania vlastností fourierovských a aproximatívnych dekonvolučných metód možno doporučiž prednostné použitie fourierovských metód. Problémy so stabilitou fourierovej transformácie, vzorkovaním, aliasingom a podobne je vhodné pritom riešiž interaktívne s grafickou analýzou výsledných profilov pri jednotlivých krokoch dekonvolučnej metódy. Aplikovanie aproximatívnych dekonvolučných metód je jednoduchšie len zdanlivo, vyžaduje taktiež veľký objem spracovaných dát pri aproximácii jednotlivých difrakčných profilov a ich charakteristík. Výsledkom týchto metód navyše nie je priamo fyzikálny difrakčný profil ale len niektoré jeho charakteristiky.

SOME OF THE PHYSICAL, PHYSICO- CHEMICAL AND TECHNOLOGICAL PROPERTIES OF POWDER MATERIALS AND THEIR RELATION TO THE X-RAY DIFFRACTION

Jiří Had

Institute of Chemical Technology, Central Laboratories, Technická 5, 166 28 Prague.

Specific density can be determined by the X-Ray diffraction from the lattice parameters and mass of the elementary cell. It has some advantages from the density bottle determination.

Bulk volume affects sample preparation. Samples with high bulk volume have lower sample consumption.

Specific surface. Powders with specific surface usually have high bulk volume and affect sample preparation in similar way.

Moisture content ought to be regarded with quantitative phase analysis. Not considerate it means to lower precision of analysis. There is also trouble with some moisture samples preparation. Moisture during the measurement is escaping and the sample can be spilled.

Surface character impact on originating of static electricity which can make some troubles with sample preparation.

Surface treatment affects character of the surface. It serves for hydrophobization or hydrophilization of the surface. Its content is usually low, layer on the particle surface is thin and in such way is not detectable by X-Ray diffraction. High surface treatment can affect results of quantitative phase analysis.

Sieve residue can be determined in watered way on the sieves of 0,063 or 0.040 mm mesh. X-Ray diffraction can distinguish if the residue consists of primary particles or aggregates of them.

Morphology of particles is related to the texture and in such way impacts on results of quantitative and in some extend even on qualitative phase analysis.

Particle size distribution is determined with the help of optical or sedimentation methods. X-Ray diffraction can catch the large particles from the film detection and the small ones from the diffraction line broadening.

Dispersibility is defined as degree of grinding in certain binding agent. It is determined with grindometer. X-Ray diffraction can sometimes help with explanation of bad grinding.

Content of water soluble salts. This content is mostly too low for X-Ray diffraction. However, evaporation residue can be used for qualitative phase analysis.

Colour is a psychosensoric quantity. It is determined by spectral reflectivity of the surface and by the spectral sensitivity of human eye in the range of visible radiation. Being mentioned in databases, colour can help in phase identification, however sometimes it is misleading. Even small amount of a substance with strong tinting strength can change sample colour. Colour of powders can be influenced by the moisture. Wet powders are darker and with larger saturation than the dry ones.

Rheological properties of suspensions have impact on the way of X-Ray measurement of suspensions and pastes and choice of goniometer type. As for suspensions with lower viscosity, vertical sample holder and steady sedimentation state or stirred cuvette is suitable.

For suspensions with high viscosity or for pastes, sample holders in vertical position and theta –theta goniometer is recommended. As for no-newtonian suspensions, thixotropy and slip yield value play a role.

TEXTURES OF ALUMINIUM ALLOY THIN SHEETS FOR HEAT EXCHANGER FINS

J. Marek, M. Karlík[1], P. Sláma[2]

[1]*Department of Solid State, Faculty of Nuclear Sciences and PhysicalEngineering, Czech Technical University in Prague, Trojanova 13, 120 00Prague 2, Czech Republic, V Holešovickách 2, 180 00 Praha 8,*
E-mail: marek@troja.fjfi.cvut.cz

[2]*Department of Materials, Faculty of Nuclear Sciences and Physical Engineering, Czech Technical University in Prague, Trojanova 13, 120 00 Prague 2, Czech Republic*

[3]*Research Institute for Metals Ltd., Panenské Brežany, 250 70 Odolena Voda*

Texture analysis of different sheets from $Al_{1.5}FeMnSi$ (AA 8006) and AlFeSi (AA 8011) alloys was carried out in order to compare textures of materials for heat exchangers fabricated by several producers and by different technologies. The textures were determined by X-ray back reflection goniometric method using SIEMENS diffractometer.

A majority of samples exhibit recrystallization R-texture, remaining sheets have a cubic texture or a combination of both texture types. Several samples, fabricated by different technologies, have a texture of the same type. Consequently it is not possible to predict the type of the texture from the technology of casting and downstream processing.

PŘÍSPĚVEK K METODICE STUDIA ELASTICKÉHO CHOVÁNÍ POLYKRYSTALŮ

N. Ganev, H. Lauschmann, I. Kraus

Fakulta jaderná a fyzikálně inženýrská ČVUT v Praze, Břehová 7, 115 19 Praha 1

Cílem příspěvku je prezentovat metodu stanovení rentgenografických elastických konstant polykrystalických materiálů používanou na Fakultě jaderné a fyzikálně inženýrské ČVUT v Praze. Možnosti tohoto experimentálního postupu jsou ilustrovány měřením rentgenografické elastické konstanty $(\frac{1}{2}s_2)^{rtg}$ [1] souboru vzorků korundové kompaktní keramiky.

Úvod
Výsledky určování napětí krystalové mřížky metodou rentgenové tenzometrie jsou ovlivňovány elastickou anizotropií, projevující se směrovou závislostí elastických vlastností. U mechanických měření deformace, kde se jedná zpravidla o objemy s velkým počtem náhodně orientovaných krystalků, je efekt anizotropie „zprůměrován" a chování objektů lze považovat za kvaziizotropní, dostatečně dobře popsatelné elastickými konstantami E, ν lineární teorie elasticity izotropních látek. Při rentgenografickém měření zbytkových napětí je elastická anizotropie respektována pomocí tzv. rentgenografických elastických konstant, jejichž hodnoty lze buď vypočítat teoreticky, nebo určit experimentálně na základě měření mřížkových deformací ve vzorcích vystavených známému jednoosému namáhání (zpravidla tahu nebo ohybu).

Zkoumané objekty korundové kompaktní keramiky
Analyzované destičky ($37 \times 10 \times 0,35$) mm^3 byly připraveny z mikrozrnného prášku U308 (99,5 % α-Al_2O_3) lisovaného při třech různých tlacích (30 MPa, 50 MPa a 80 MPa) a následně slinutého při teplotách 1550 °C, 1600 °C a 1680 °C.

Použité experimentální metody
Makroskopické elastické konstanty byly měřeny při statickém tříbodovém ohybu nosníku, resp. desky. Metoda vychází z lineární závislosti průhybu na zatížení. K tomuto účelu byl navržen a vyroben zvláštní přípravek. Zatěžování se realizuje sadou závaží, průhyb je měřen metodou ostření obrazu na metalografickém mikroskopu. Reálná přesnost stanovení Youngova modulu pružnosti E je cca ± 3 %.
Mřížkové deformace byly měřeny pomocí speciálního přípravku k provádění zkoušek čistým ohybem na rtg gonio-

metru Siemens. Průhyb vzorku se nastavuje podle údaje na úchylkoměru. Konstrukce umožňuje vrátit celý držák zpět, takže vzorek zůstává i po deformaci v ose goniometru. Byla použita rentgenka s Cu anodou a při postupném zatěžování zkoumaných vzorků detekována difrakční linie {40.10} α-Al_2O_3.

Výsledky

Podmínky přípravy analyzovaných vzorků a experimentálně zjištěné makroskopické (E_{mech}) a rentgenografické ($\frac{1}{2}s_2$) elastické konstanty jsou shrnuty v následující tabulce.

Vzorek	LT, MPa	ST, °C	Tloušžka, mm	E_{mech}, GPa	$\frac{1}{2}s_2.10^6$, MPa^{-1}
17M1	30	1680	0,329	357	2,20 ± 0,10
16M1	30	1600	0,355	383	2,03 ± 0,21
15M2	50	1550	0,363	355	2,23 ± 0,13
17M2	50	1680	0,348	368	2,08 ± 0,13
16M2	50	1600	0,333	407	2,44 ± 0,14
16M3	80	1600	0,348	423	2,39 ± 0,33

LT … lisovací tlak, ST … slinovací teplota

Chyba stanovení Youngova modulu E_{mech} byla cca 3%, uváděna přesnost stanovení $\frac{1}{2}s_2$ představuje standardní odchylku odhadu parametru lineární regrese.

Závěry

1. Průběh závislosti E_{mech} na lisovacím tlaku má rostoucí tendenci.

2. Hodnoty stanoveného makroskopického Youngova modulu pružnosti E se u jednotlivých měřených vzorků liší v rozmezí 355 - 423 GPa, a jsou tedy až o 20 % vyšší než obvykle udávaná hodnota E = 350 GPa [1, 2].

3. Chyba stanovení rentgenografické elastické konstanty $(\frac{1}{2}s_2)^{rtg}$ se pohybovala v rozmezí 5 až 6 % s výjimkou dvou vzorků, u nichž dosáhla cca 10 – 13 %.

4. Rozdíly experimentálně stanovených hodnot $(\frac{1}{2}s_2)^{rtg}$ jsou u analyzovaných vzorků statisticky nevýznamné a jejich střední hodnota $<\frac{1}{2}s_2> = 2,23.10^{-6}$ MPa^{-1} je nižší než běžně uváděné hodnoty $\frac{1}{2}s_2 = (3,07 – 3,70).10^{-6}$ MPa^{-1} [1, 2].

Literatura

1. Kraus I., Ganev N.: Difrakční analýza mechanických napětí. Skripta ČVUT. Nakladatelství ČVUT. Praha 1995.

2. Eigenmann B.: Röntgenographische Analyse der inhomogenen Spannungszustände in Keramiken, Keramik-Metall-Fügenverbindungen und dünnen Schichten, Dissertation, Universität Karlsruhe 1990.

ANALÝZA ROZHRANIA SPÁJKY AG800 S NITRIDOVOU KERAMIKOU

Ľ. Čaplovič[1], M. Čaplovičová[2], V. Pulc[3] a J. Krištín[2]

[1]*Katedra materiálového inžinierstva, Materiálovotechnologická fakulta STU, 917 24 Trnava, Slovenská republika*

[2]*Centrálne laboratóriá elektrónovooptických metód, Prírodovedecká fakulta UK, 842 00 Bratislava, Slovenská republika*

[3]*Katedra materiálov a technológií, Strojnícka fakulta STU, 812 32 Bratislava, Slovenská republika*

Použitie konštrukčnej keramiky pri výrobe zložitých a extrémne zažažených strojov a zariadení je ovplyvnené radom technologických faktorov. Vzhľadom na jej prirodzenú krehkosž, ako aj náročný spôsob výroby zložitých kompaktov je výhodné vytváraž kombinované spoje keramiky s kovmi a zliatinami kovov. Tým sa v maximálnej miere využije ich mimoriadna odolnosž proti teplotným vplyvom a potlačia nepriaznivé krehkolomové charakteristiky. Jednou z metód používanou v súčasnosti na zhotovenie kombinovaných kovokeramických materiálov je technológia spájkovania pomocou aktívnych spájok.

Konštrukčná keramika na báze Si_3N_4 patrí medzi najstabilnejšie zlúčeniny a v procese spájkovania sa zmáča iba v dôsledku chemickej reakcie so spájkou, ktorá obsahuje prísadové prvky ako Ti, Zr, Be, In aktivizujúce tento proces. Takto zhotovený spoj je v prevádzke väčšinou vystavený dlhodobým teplotným vplyvom, ktoré ho môžu za istých podmienok degradovaž vznikom nežiadúcich fáz na rozhraní spájka-keramika. Z tohto dôvodu je nutné poznaž teplotnú stabilitu rozhrania.

Pre experimenty sa použila konštrukčná keramika na báze Si_3N_4 (84,1 hm.% Si_3N_4; 10,6 hm.% Y_2O_3; 5,3 hm.% Al_2O_3), na ktorú bola vo vákuu pri teplote 900°C/30 min nanesená vrstva aktívnej spájky Ag 800 (72 hm.% Ag; 26,5 hm.% Cu; 1,5 hm.% Ti). Takto získané vzorky boli potom teplotne exponované pri teplote 715 °C s výdržou 42,5 a 100 hodín.

Na všetkých vzorkách sa vykonala rtg. difrakčná fázová analýza na rtg. difraktometri DRON 3M (Cu-anoda, sekundárny monochromátor LiF) a to tak, že sa postupne zbrusovala vrstva nanesenej spájky až do rozhrania s keramikou. Súčasne sa na priečnych rezoch zmerali čiarové koncentračné profily prvkov zúčastnených na vytvorení spoja (Ag, Si, Ti, Cu) pomocou VDA mikroanalyzátora.

Výsledky experimentov ukázali, že na rozhraní spájka - keramika sa vytvorila reakčná medzivrstva obohatená titánom s hrúbkou 3 až 5 m, v ktorej sa zistila prítomnosž zlúčenín na báze titánu ($CuTi_2$, $AgTi_3$, $TiSi_2$ a TiN). Ich vzájomný pomer sa aj po dlhodobej teplotnej expozícii menil iba minimálne.

Podobne sa nepozorovala ani pôvodne predpokladaná výrazná migrácia atómov titánu cez rozhranie do konštrukčnej keramiky a tým následná degrádacia spoja v dôsledku rozpadu fázy Si_3N_4 a vznikom nitridov titánu.

Celkovo možno konštatovaž, že dlhodobá expozícia rozhrania spájka Ag 800 – keramika na báze Si_3N_4 iba minimálne ovplyvňuje kvalitu spájkovaného spoja.

LECTURES - 21. 6.

DIFFUSE SCATTERING OF X-RAYS

Jaroslav Fiala

New Technologies Research Center, University of West Bohemia, Universitní 22, 30614 Plzeň, Czech Republic

The success of the structural crystallography is due to the fact that crystals consist of three-dimensional arrays of almost identical units, which gives rise to diffraction patterns consisting of discrete diffraction peaks (Bragg reflections). Real materials, however, only approximate this ideal, and their diffraction patterns contain, in addition to sharp Bragg peaks, a weak continuous background known as diffuse scattering. This scattering contains very detailed information on the microscopic structure of defects in crystalline solids. Such defects, i.e. departures from ideality, may arise in a whole variety of different ways and to different extents, strongly affecting and even determining mechanical, electrical and other properties of many materials. That is why X-ray diffuse scattering has long been of interest as a tool for examining the relationships between the materials structure and properties. In this contribution, the general equations for X-ray diffuse scattering are derived and the methods for employing these equations to identify the various structural features of the material under consideration are discussed.

LATTICE IMAGING IN TRANSMISSION ELECTRON MICROSCOPY

Miroslav Karlík

Department of Materials, Faculty of Nuclear Sciences and Physical Engineering, Czech Technical University in Prague, Trojanova 13, 120 00 Prague 2, Czech Republic, E-mail: karlik@kmat.fjfi.cvut.cz

With the resolution becoming sufficient to reveal individual atoms, high-resolution electron microscopy (HREM) can now compete with X-ray and neutron methods to determine quantitatively atomic structures of materials, with the advantage of being applicable to non-periodic objects such as crystal defects. An introduction to the theory and practical aspects of HREM is given. Principles of other lattice imaging techniques in transmission electron microscopy – electron holography and Z-contrast imaging are also described.

The last decades are characterized by an evolution from macro- to micro- and more recently to nanotechnology. Examples are numerous, such as nanoparticles, nanotubes, quantum transistors, layered superconducting and magnetic materials, etc. Since many material properties are strongly connected to the electronic structure, which in turn is considerably dependent on the atomic positions, it is often essential for the materials science to determine atom positions down to a very high precision. Classical X-ray and neutron techniques fail for this task, because of a non-periodic character of nanostructures. Only fast electrons are scattered sufficiently strongly with matter to provide local information at the atomic scale.

One of the most commonly used high-resolution techniques in transmission electron microscopy (TEM) is that of (bright-field) phase-contrast imaging. This relies on the interference between beams scattered by a specimen and is usually performed under parallel beam illumination conditions. The main, and significant, disadvantage of this lattice imaging method is in the difficulty of interpreting an image in terms of the atomic structure of the specimen. The interpretation is carried out using computer simulations requiring input of a model of specimen structure, specimen thickness and microscope parameters.

Unfortunately, even the best electron microscopes are hampered by the fact that only the intensity (i.e. the squared amplitude), of the electron wave can be recorded on the photographic film or CCD-camera and an essential part of the electron wave, the phase information, is lost. Holographic recording overcome this problem. The (aberrated) image wave is superimposed with an unscattered plane reference wave resulting in an interference pattern - electron hologram. After acquisition and transfer to a computer system, amplitude and phase of the electron wave are reconstructed using the laws of Fourier optics by sophisticated image processing. Electron – specimen interaction is then simulated in the same manner as in the case of conventional phase-contrast imaging.

On the other hand the Z-contrast technique provides directly interpretable images - maps of scattering power of the specimen. Allowing incoherent imaging of materials, it represents a new approach to high-resolution electron microscopy. The Z-contrast image is obtained by scanning an electron probe of atomic dimensions across the specimen and collecting electrons scattered to high angles. In parallel, spectroscopic techniques can also be used to supplement the image, giving information on atomic-resolution chemical analysis and/or local electronic band structure. The resolution of the technique is determined by the size of the electron probe.

This paper gives an introduction to the theory and practical aspects of high-resolution electron microscopy. Principles of electron holography and Z-contrast imaging are also described.

POSITRON ANNIHILATION SPECTROSCOPY (PAS)

Ivan Procházka

Department of Low Temperature Physics, Faculty of Mathematics and Physics, Charles University in Prague, V Holešovičkách 2, CZ-180 00 Praha 8, Czech Republic

PAS involves several experimental techniques purposed for investigations of annihilation of electron (e^-) – positron (e^+) pairs. Nowadays, PAS is widely recognised as an effective method of condensed matter studies and materials research.

In conventional PAS, artificial β^+ emitters, like e.g. ^{22}Na, are used as positron sources. When an energetic positron is implanted into a medium it quickly reaches thermal equilibrium with its surroundings. During thermalisation, the kinetic energy of the positron is dropped from its initial value of $\sim 10^2$ keV below to $\sim 10^2$ meV. Despite of such a colossal change of energy, the thermalisation times in most substances are as short as a few ps. The thermalised positron diffuses through the medium as a free particle, which diffusion motion is characterised with a diffusion length of $\sim 10^2$ nm. Eventually, the positron annihilates with an electron of the medium. The total energy of the annihilating $e^- - e^+$ pair is transferred to annihilation photons γ created in this process. Usually the two-photon annihilation, $e^- + e^+ \rightarrow 2\gamma$, is the only significant channel of the $e^- - e^+$ annihilation reaction in a medium.

Due to the Coulomb repulsion with positive atomic cores at lattice sites, positrons prefer to reside in the inter-atomic space. Absence of this repulsion at the open volume defect sites (e.g. vacancies, dislocations, few-vacancy clusters etc.) can make these sites capable of positron trapping. If such centres are present in the medium a certain fraction of thermalised positrons may get captured there before annihilation which constitutes a basis for defect studies by means of the PAS method.

In many insulators, the positron can form a bound state with a host electron, positronium (Ps), which is an analogue of the hydrogen atom. Ps exists in the singlet (parapositronium, pPs) or the triplet (orthopositronium, oPs) state. While the two-photon self-annihilation of pPs is an allowed process, the two-photon annihilation of oPs can proceed only via the pick-off reaction with an electron of the host. Due to exchange interaction of its electron with environmental electrons, Ps atom is repelled to an unoccupied space in the material.

Basic measurable parameters of the two-photon $e^- - e^+$ annihilation of the $e^- - e^+$ pair are (i) the positron annihilation rate (or the positron lifetime), (ii) the Doppler shift of the annihilation-photon energy, arising from movement of the annihilating pair at the moment of annihilation and (iii) the angular correlation between the two annihilation photons. Applicability of PAS to materials studies is substantiated by the fact that the structure of the medium is reflected in the above PAS parameters. There are the two ways how the dependencies of these parameters on the medium structure arise: (i) Through the state of the electron participating in the annihilation reaction. This introduces dependence on the local electronic structure of the host at the annihilation site. (ii) Through the state of the positron itself at the moment of annihilation: the free positron, positron captured at a trap or different states of the Ps atom in the medium. The state reached by the positron at the time of annihilation is a result of positron interactions in the medium prior to annihilation.

Range of the energetic positrons in matter amounts typically > 0.1 mm. Conventional PAS thus probes bulk properties of condensed matter. Recent development of positron beams with variable energy from a few eV to keV region has made possible to extend PAS applications towards surface studies.

Among various properties of condensed matter investigated by means of PAS, electronic structure and small-size defects are those which have been most extensively studied up to now. It is a significant advantage of PAS that the defects of the size as small as that of a monovacancy can be detected and PAS appears to be sensitive at a very low defect concentrations, e.g. vacancy concentrations of $\sim 10^{-7}$ in metals. In addition, phase transformation and precipitation phenomena are frequently investigated by PAS. While positron is used as a probe in investigations of e.g. metals and semiconductors, Ps atoms play a role of the main probe in PAS studies of free volume in polymers. Number of different applications of PAS to polymer materials is rapidly growing at present.

In the present lecture, fundamental features of PAS will be reviewed. Experimental arrangement built in positron laboratory at Charles University in Prague will be described. Several examples of PAS applications will be given. These examples will cover the three main classes of materials which are currently being extensively investigated by PAS: metallic systems, semiconductors and polymers.

VYUŽITIE CBED PRI URČOVANÍ BODOVÝCH GRÚP KRYŠTÁLOV

M. Čaplovičová[1]

[1]Centrálne laboratórium elektrónovo-optických metód, Prírodovedecká fakulta UK, 842 15 Bratislava, Slovenská republika

Pri metóde CBED (Convergent Beam Electron Diffraction) sa na vyčlenenie oblasti, ktorá prispieva k difrakčnému obrazu, využíva konvergentný lúč elektrónov. CBED obrazy sú tvorené sériou krúžkov, pričom každý z nich odpovedá inej rovine, pre ktorú je splnená Braggova difrakčná podmienka. Zmeny intenzity vo vnútri krúžkov sú dané symetriou kryštálu a sú funkciou uhla medzi dopadajúcimi elektrónmi a konkrétnym smerom v kryštáli. Sú nositeľmi informácií o bodovej symetrii kryštálov, o orientácii vzorky, o jej hrúbke atď. CBED sa využíva pri identifikácii fáz, pri určovaní bodových a priestorových grúp kryštálov, hrúbky kryštálov, mriežkových parametrov, vnútorných napätí a pod. Rozlišovacia schopnosž CBED je väčšia ako v prípade SAED (Selected Area Electron Diffraction). Excitovaný objem môže maž priemer len 1nm.

Pri určovaní symetrie kryštálov pomocou CBED je možné využiž viacero metód (beam-rocking method, signal processing method, LA CBED (Large-Angle CBED), hollow-cone beam method [1]. Z nich sa najviac využíva metóda LA CBED. Bodová rovinná symetria kryštálu sa stanovuje na základe symetrie rozloženia intenzity v difrakčných krúžkoch a zodpovedá niektorej z desiatich dvojrozmerných bodových grúp.

Pri štandardnej metóde určovania bodových grúp podľa Buxtona a kol. [2] sa vychádza zo symetrie štyroch LA CBED obrazov (symetria celkového CBED obrazu, symetria centrálneho krúžku, symetria obrazu difraktovaného lúča a symetria páru difraktovaných lúčov). Jednoduchší prístup pri určovaní bodových grúp zvolil Tanaka a kol. [1], ktorý pre tento účel navrhli metódu viaclúčovej difrakcie. Na stanovenie bodovej grupy kryštálov postačuje iba jeden CBED obraz.

Ako príklad pre stanovenie bodovej grupy bol vybraný monokryštál kremíka. Difraktovaná intenzita v centrálnom krúžku v smere o vykazuje symetriu *3m*. Symetria celého CBED obrazu so zónovou osou o je taktiež *3m*. Ak sú v reflexnej polohe roviny (2$\bar{2}$0) a ($\bar{2}$20) difraktovaná intenzita má symetriu *m*. V prípade, že kryštál Si je orientovaný v smere d, centrálny krúžok a celkový CBED obraz majú symetriu *4mm*. Distribúcia intenzity v krúžkoch patriacich difraktujúcim rovinám (400) a ($\bar{4}$00) má symetriu *2mm*. Pomocou grafických schém a pomocou tabuliek uvedených v [2] a na základe uvedených údajov, je možné jednoznačne stanoviž bodovú grupu ako *m3m*.

Ak z údajov o distribuovanej intenzite v centrálnom krúžku a difrakčných krúžkoch nie je možné jednoznačne stanoviž bodovú grupu, je potrebné urobiž CBED obraz v smere inej zónovej osi.

1. M.Tanaka & M.Terauchi, *Convergent Beam Electron Diffraction*, (1985), pp.192

2. B.F.Buxton et al., *Phil. Trans. R. Soc.,* London, 281, (1976), 181

Chemistry

CONFORMATIONAL FLEXIBILITY OF CYCLOSPORINS

B. Kratochvíl[1], M. Hušák[1] and A. Jegorov[2]

[1]*Department of Solid State Chemistry, Institute of Chemical Technology, 166 28 Praha 6, Czech Republic*

[2]*IVAX CR-GALENA, Research Unit, 370 05 České Budějovice, Czech Republic*

Natural cyclosporins are cyclic undecapeptides produced biotechnologically by submerged fermetation of the genus *Tolypocladium*. Immunosuppressive cyclosporin A, (CsA = cyclo (-MeBmt[1]-Abu[2]-Sar[3]-MeLeu[4]-Val[5]-MeLeu[6]-Ala[7]-D-Ala[8]-MeLeu[9]-MeLeu[10]-MeVal[11]-)), Figure1., is therapeutically used in transplantation surgery (e.g. *Neoral*, Novartis or *Consupren*, Galena).

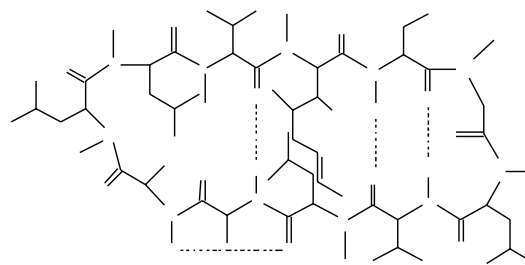The other cyclosporins are derived from Cs A by the re-

Figure 1. Cyclosporin A

placement of usually one or two of its amino acids. They are denoted as Cs B…Cs Z or by description of substitution, e.g. [Ala[2]] Cs A. Non-immunosuppressive cyclosporins are also biologically active compounds, some of them maybe with distinct potential for the treatment of multidrug resistance of tumor cells.

An explanation of the biological activity of cyclosporins is based on the conformational flexibility of their molecular skeleton. The present study deals with conformations of crystalline cyclosporin clathrates.

Cyclosporin clathrates are compouds in which cyclosporin molecules are associated *via* van der Waals forces and forming cavities occupied mostly by solvent molecules. The chirality of cyclosporin skeleton, disymmetry of cavities and H-bridges forming among the guest solvent molecule and atoms of cavity gives possibility to use the preferential crystallization for the separation of different enantiomers. These phenomena can be best exemplified just on the example of different arrangement of one of two tert-butyl methyl ether molecules in Cs V and dihydro-Cs A clathrates.

Further, it has been found that a relatively high conformational stability of cyclosporin molecules in crystalline state causes the preference of the definite symmetrical arrangements. The two main symmetries were identified for cyclosporin clathrates: space groups $P2_1$ and $P2_12_12_1$. Large cavities (391 – 562 Å^3) were localized in cyclosporin clathrates of the $P2_1$ symmetry with Z=2, small cavities (about 20 Å^3) are typical for cyclosporin structures of the $P2_12_12_1$ group crystallizing without solvent (e.g. acetyl-Cs A) or with water molecule only (e.g. Cs A . $2H_2O$).

NEOBVYKLÉ METODY VISUALISACE STRUKTURNÍCH DAT

M. Hušák

VŠCHT Praha

V některých případech je velice komplikované interpretovat mapy elektronové hustoty automaticky. Standardní 2D mapa někdy pro pochopení toho , co se vlastně ve zkoumané části prostoru nachází, nestačí. Pro lepší zobrazení map elektronových hustot, ale i dalších silových polí, byly testovány následující techniky: stereoskopické zobrazení pomocí LCD brýlí, stereoskopické zobrazení pomocí náhlavního displej (HMD) kombinovaného s zahrnutím sledování pozice uživatele do scény a použití komplexního VR projekčního prostředí CAVE.

Tvorbu obrazu pro výše zmíněná zařízení zajišžuje experimentální program MCE_VR, který je přímo schopný číst výstupní data z krystalografického programu CRYS-TALS a s pomocí WinGX interface i z programu SHELX. Program používá pro tvorbu grafiky hardwarové urychlení pomocí standardu OpenGl. Díky použití knihovny GLUT je kód nezávislý na operačním systému. Zatím existují experimentální verze tohoto programu pro PC a SGI.

Pro testování výstupu do HMD bylo použito zařízení VFX3D firmy IIS. Vývoj verze programu pro 3D projekční zřízení CAVE probíhá ve spolupráci s Ústavem pro paralelní zpracování dat university v Linzi, který k tomuto zařízení umožnil přístup.

SWAXS MEASUREMENTS ON POLYMERS AND BIOPOLYMERS AT ELEVATED PRESSURES

M. Steinhart[1], M. Kriechbaum[2], H. Amenitsch[2], S. Bernstorff[3], P. Laggner[2], J. Baldrian[1] & R. Triolo[4]

[1]Institute of Macromolecular Chemistry, Academy of Sciences of the Czech Republic, Prague

[2]Institute of Biophysics and X-Ray Structure Research, Austrian Academy of Sciences, Graz

[3]Sincrotrone Elettra, Trieste, Italy

[4]Dipartimento di Chimica-Fisica, Universitŕ di Palermo, Italy

An instrument to facilitate small- and wide-angle X-ray scattering measurements of phenomena induced in samples by elevated hydrostatic pressure as well as by pressure variations including jumps has been constructed [1, 2] and is being used for several kinds of experiments [3].

A pressure range from atmospheric up to 0.25 GPa (2.5 kbar) can be employed. The pressure is transferred by means of pressurising medium (liquid or gaseous) to an X-ray sample cell. The cell has two Beryllium or diamond windows. The former have high transmission (0.4), the latter on the other hand show considerably lower background scattering. Scattering curves can be observed at angles up to 30°. The sample consistency can range from solid to liquid with a minimal volume less than 30 µl and an irradiated volume up to 3 µl with an optical path-length ranging from 0.5 up to 4 mm. The pressurising medium can be separated from the sample by several ways thereby providing suitable environment for the particular sample.

The device is fully PC controlled and is capable of being integrated into a channel control and data acquisition system at a high-flux synchrotron facility. Static measurements at elevated pressures and in addition time-resolved experiments with the time resolution down to the milliseconds range can be performed.

Among the problems studied recently with the use of the high pressure instrument the most important are barotropic phase transitions in lipid/water systems (DOPE, DPPC), pressure induced crystallizations of polymer blends (PEO, PMMA) and investigations of aggregation phenomena of block co-polymers in supercritical CO_2. Beside measurements on bulk samples also grazing incidence experiments using silicon wafer with highly aligned samples are carried out.

More detailed description of the high-pressure instrument and mainly some interesting results of the particular studies will be presented in the talk.

1. K. Pressl, M. Kriechbaum, M. Steinhart, and P. Laggner, *Rev. Sci. Instrum.*, **68**, 4588-4592 (1997).

2. M. Steinhart, M. Kriechbaum, K. Pressl, H. Amenitsch, P.Laggner, and S. Bernstorff, *Rev. Sci. Instrum.*, **70**, 1540-1545 (1999).

3. see Annual Report of the Austrian SAXS Beamline at Elettra, Trieste (1996-7, 1998,1999)

APPLICATION OF BOND-VALENCE THEORY TO STRUCTURES OF COORDINATION COMPOUNDS

F. Valach[1], M. Tokarčík[1], T. Maris[2], A. Saunders[2], A. Cowley[2], D. J. Watkin[2] and C. K. Prout[2]

[1]Department of Chemical Physics, Faculty of Chemical Technology, Slovak University of Technology, Radlinského 9, 812 37 Bratislava, Slovak Republic.

[2]Chemical Crystallography Laboratory, 9 Parks Road, Oxford, OX1 3PD, England.

Bond valence quantity as the function of inter-nuclear distance in the form $s = a_1/r + a_2/r^2 + a_3/r^3 + a_4/r^4 + a_5/r^5$ was developed [1]. The a_i parameters were estimated via

minimization of the function $\sum (Z_k - V_k)^2$. Z_k are oxidation numbers of central atoms and V_k are their bond-valence sums. The inter-nuclear metal-ligand distances of Cambridge Structural Database System [2] and Inorganic Crystal Structure Database [3] were used in minimization procedure. Based on the developed bond-valence theory mutual dependence between the bond length in copper coordination sphere with chromophore CuN_2O_4 has been derived and compared with the experimental structural correlations. Nonbonding character of inter-nuclear Cu(II)...Cu(II) contact in 26 binuclear carboxylic complexes [4] and 9 binuclear propionates [5] is consistent with bond-valence sum model . If the contribution of basal Cu-O, N bonds to the bond valence sum around the central atom is known the remaining bond length of inner coordination sphere can be predicted by derived formula. The predicted Cu(II)-O bond length of [Cu_2(2-fluorobenzoate)$_4$ (2-fluorobenzoicacid)$_2$] [6] is 2.16 Å . Observed Cu-O bond length is 2.193(2) Å. Semicoordination in Cu(2-Cl-6-FC$_6$H$_3$COO)$_2$ (nicotinamide)2 complex [7] and chelation of Cu(II) ion in [Cu(CH$_3$CH$_2$COO)$_2$ (methyl 3-pyridyl-N-carbamate)$_2$] 0.25 [8] was proved. For the high temperature Ba$_2$YCu$_3$O$_x$ superconductors the linear correlation [d(Cu-O)/r$_L$(max)]$_{vs.}$ Tc was estimated. d(Cu-O) is out-of-plane copper-oxygen bond length of the copper atom coordination sphere and Tc is transition temperature of superconductor. r$_L$(max) is supreme limit of Cu-O distance which should still be considered as chemical interaction.

1. F. Valach, Polyhedron 18 (1999) 699.

2. F. H. Allen, O. Kennard, Chem. Design Automation News. **8** (1993) 31.

3. Gmelin Institut für Anorganische Chemie und Fachinformationszentrum FIZ Karlsruhe, Germany, 2000.

4. F. Valach, M. Tokarčík, T. Maris, D. J. Watkin &C. K. Prout, *J. Organometallic Chem.* **622** (2001) 166.

5. F. Valach, M. Tokarčík, A. Saunders, A. Cowley & D. J. Watkin, *Polyhedron* (2001). In press.

6. F. Valach, M. Tokarčík, T. Maris, D. J. Watkin & C. K. Prout, *Z. Kristallogr.* **215** (2000) 56.

7. N. N. Hoang, F. Valach & M. Dunaj-Jurčo, *Acta Cryst.* **C51** (1995) 1095.

8. M. Koman, M. Melník, & T. Glowiak, *Acta Cryst.* **C54** (1998) 1604.

Biology, Macromolecular Chemistry

PROTEINOVÁ KRYSTALOGRAFIE V POSTGENOMICKÉ ÉŘE

Jaromír Marek[1]

[1]*Laboratoř funkční genomiky a proteomiky, Přírodovědecká Fakulta, Masarykova univerzita v Brně, Kotlářská 2, 611 37 Brno, e-mail:marek@chemi.muni.cz*

V únoru letošního roku bylo oznámeno, že v rámci mezinárodní spolupráce mnoha různých vládních organizací i soukromých společností bylo dokončeno určování primární struktury lidského genomu, a jen několik týdnů či měsíců před tím byly zveřejněny i první úplné genetické sekvence rostliny, hmyzího jedince a živočicha. Po postupném utišení nadšení redaktorů denního tisku nad tím, že „známe kód, podle kterého funguje člověk", se ukazuje, že určení primární struktury DNA je jen úvodní krok ve směru k pochopení smyslu a funkce genetické informace, a že za ním budou muset nutně následovat i kroky další.

Logicky nejbližším následujícím cílem vědy v tomto směru zřejmě bude určování jednotlivých genů pomocí DNA kódovaných (v tento okamžik např. není ani přesně známo, kolik jich v lidské DNA může být, odhaduje se jen, že půjde o počet někde mezi 33 a 50 tisíci) a studium struktury a funkcí jejich jednotlivých produktů – enzymů. Jako pokračování *Human genome* projektu v *postgenomické* éře se proto v zahraničí mluví o *Human proteome project* – o projektu pro určení struktur všech lidských enzymů.

Pro určování struktur enzymů se v současnosti používají dvě hlavní experimentální metodiky – metoda nukleární magnetické rezonance (NMR) a rentgenová proteinová krystalografie (X-ray). PDB, databáze 3-D proteinových struktur, v současnosti obsahuje něco přes 12 tisíc položek určených pomocí X-ray a kolem 2 a 1/4 tisíce množin NMR struktur, a mezi odborníky se předpokládá, že přibližný poměr 5:1 v množství výsledků dosažených pomocí X-ray a NMR s majoritou u difrakčních metod zůstane zachován i v nejbližší budoucnosti.

Očekávaný výrazně vyšší výstup, který budou v rámci proteomického projektu biochemikové, genetikové a molekulární biologové v nejbližší budoucnosti od světové komunity krystalografů požadovat, vedl v posledních letech k velmi rychlému metodickému i instrumentálnímu rozvoji proteinové krystalografie. Cílem přednášky je podat stručný přehled o hlavních výsledcích a trendech tohoto vývoje, a případně i vyvolat diskusi na téma, co takovýto vývoj může znamenat pro proteinovou krystalografii v ČR.

STRUCTURAL STUDY OF PROTEINS

J. Ševčík and Ľ. Urbániková

Institute of Molecular Biology, Slovak Academy of Sciences, 84251 Bratislava, Slovak Republic

Determination of protein structures has became extremely important as it gives a new dimension to molecular biology. Detailed knowledge of tertiary structure of proteins is essential for understanding their function in various biological processes and for modifying their properties using protein engineering techniques which is required by food industry, biotechnology, pharmacology, medicine, etc. The sequences of human genome and those of various model organisms and many important microbial pathogens prompts an important initiative in structural genomics which is concerned with the systematic analysis of the three-dimensional structure of proteins and aims at a complete structural description of a defined set of molecules. It is expected that structural genomics will yield tens of thousands of experimental protein structures and an even larger number of calculated comparative protein structures. This enormous amount of structural data will accelerate scientific discovery in all areas of biological science, including biodiversity and evolution in natural ecosystems, agricultural plant genetics, breeding of farm and domestic animals, and, the most important, human health and disease.

There are about 13,000 structures in Protein Data Bank at present. The number is increased each year by about 1,000 structures and this accelerates every year. However, there are only 700 structures with unique polypeptide folds, the rest are similar structures of proteins from other organisms, structures of complexes, mutants etc. Estimations predict 1,000 - 5,000 unique polypeptide chain folds in nature. Based on the sequence of amino acids, function and structure, proteins can be grouped into families. Each newly determined unique structure typically provides useful structural information for a family of 15 - 40 protein sequences for which no structural data were previously available. Comparative, or homology modelling (*in silico*) is currently restricted to protein sequences for which a similar experimental template, defined by amino acid sequence identity higher than 30 - 35 %, is available. Current estimates suggest that a structural study focussing on 10,000 - 20,000 selected proteins will yield a complete ensemble of protein structures which will enable homology modelling of every globular segment of every protein found in nature.

Structural study of proteins at our Institute started about 20 years ago. At that time the overall situation concerned with necessary environment was not quite favourable, at least in this country, for structural research of proteins. Structural study of proteins required new methods using both laboratory as well as computational techniques. Beside human potential and financial means to purchase necessary equipment it was also necessary to change the view of scientific community. At present, structural genomics is in the forefront of our scientific interest.

Determination of protein structures using diffraction techniques starts in biochemistry and molecular biology (isolation and sequencing of a protein from its native producer and/or preparation of recombinant protein, characterisation of the protein, crystallization) followed by physical and mathematical procedures (data collection, structure determination) and interpretation of the structure from the biological point of view. Among the steps of protein structure determination, there are two the most important and at the same time the most problematic: crystallization and phase determination. Obtaining suitable single crystals, which are willing to diffract to a reasonable resolution, is the least understood step based mainly on a trial-end-error procedure.

The first protein crystal in this country used for structure determination was that of ribonuclease Sa from *Streptomyces aureofaciens* which was prepared at the Institute of Molecular Biology in Bratislava. Its tertiary structure was determined at 1.8 Å resolution [1] followed by 1.7 and 1.2 Å (atomic) resolution structures [2, 3]. The structure of this enzyme at 1.0 Å resolution is prepared for publication. The structures of the RNase Sa complexes with mononucleotides contributed to better understanding of catalytic reaction mechanism, structural basis for specific recognition of substrate and structure – function relationship [1, 2, 4, 5]. Later, structures of closely related ribonucleases RNase Sa2 and cytotoxic RNase Sa3 produced by various strains of *Streptomyces aureofaciens* have been determined at high resolution. The ribonucleases were used also as model proteins in the study of conformational stability of proteins. For this study seven RNase Sa mutant structures were determined and used for estimation of a hydrogen bond contribution to the conformational stability [6,7]. Important field of study was protein – protein and protein – nucleic acid recognition based on structures of RNase Sa – inhibitor complexes. The most important structure was that of the complex of RNase Sa with barstar [8], inhibitor of a ribonuclease isolated from *Bacillus amyloliquefaciens*. As the mechanism of protein – protein recognition is one of the most important phenomena in biology, we continue in this study. We have isolated two new ribonuclease inhibitors from *S. aureofaciens* [9] and prepared several new complexes, structure determination of which is under way. We have been concerned also with structural study of amylolytic enzymes. The structure of a glucoamylase from *Saccharomycopsis fibuligera* was determined at 1.6 [10] and 1.1 Å resolution and the structure of the glucoamylase –acarbose complex at 1.6 Å. Structures of RNase Sa and glucoamylase at atomic resolution determined with very high accuracy brought new views on geometry of protein structures.

In summary, we have deposited with Brookhaven Protein Data Bank 18 structures and 10 structures are close to finalisation. The list of proteins we work on was recently widened by a glucosidase from *Termomonospora curvata*, mitochondrial processing peptidase from yeast *Sachcaromyces cerevisiae* and cytoskeletal protein plectin isolated from mouse. The crystals of these proteins were already prepared and test data sets collected.

1. Ševčík J, Dodson E.J., Dodson G.G., *Acta Cryst.,* **B47** (1991) 240-253.

2. Ševčík J., Hill C., Dauter Z., Wilson K.S., *Acta Cryst.*, **D49** (1993) 257-271.

3. Ševčík J., Dauter Z., Lamzin V.S., Wilson K.S., *Acta Cryst.*, **D52** (1996) 327-344.

4. Ševčík J., Sanishvili R.G., Pavlovsky A.G., Polyakov K.M., *TIBS* **15** (1990) 158-162.

5. Ševčík J., Zegers I., Wyns L., Dauter Z., Wilson K.S., *Eur. J. Biochem.*, **216** (1993) 301-305.

6. Hebert, E.J., Giletto, A., Ševčík, J., Urbániková, Ľ., Wilson, K.S., Dauter, Z., Pace, C.N., *Biochemistry* **37** (1998) 16192-16200.

7. Pace C.N., Hebert E.J., Shaw K., Schell D., Both V., Krajčiková D., Ševčík J., Dauter Z., Hartley R.W., Grimsley G.R., *J. Mol. Biol.* **279** (1998) 271-286.

8. Ševčík J., Urbániková Ľ., Dauter Z., Wilson K.S., *Acta Cryst* **D54** (1998) 954-963.

9. Krajčíková D., Hartley R.W., Ševčík J., *J .Bacteriol.* **180** (1998) 1582-1585.

10. Ševčík J., Solovicová A., Hostinová E., Gašperík J., Wilson K.S., Dauter Z., *Acta Cryst.* **D54** (1998) 854-866.

STUDIES OF MACROMOLECULAR SOLVATION SHELLS

J. Dohnálek, J. Hašek, J. Dušková

Institute of Macromolecular Chemistry, Academy of Sciences of the Czech Republic, Heyrovského nám. 2, 162 06 Praha 6, Czech Republic.

Solvation effects determine to great extent the formation and behavior of the three-dimensional structure of macromolecular systems. The important role of hydration in protein folding and function has been identified and discussed in the literature [1]. The growing number of determined protein and DNA/RNA structures is becoming a challenge for a systematic study of macromolecular hydration shells.

Water participates in non-specific interactions of hydrophobic and hydrophilic surfaces and in specific hydrogen bond networks [1]. Crystallographically determined hydration sites on the surface of biological molecules partially conform to the specific conditions of a given experiment (pH level, space group, varying contacts to neighboring molecules). Analysis of similar crystal structures of the same system crystallized in various space groups and physical and chemical conditions can contribute to a separation of the above named effects and to a generalization of these observations for other solvated systems.

The protease of the Human Immunodeficiency Virus (HIV), the causative agent of acquired immunodeficiency syndrome (AIDS), has been studied in complexes with many inhibitors representing potential drugs (more than 180 determined structures in the PDB database [2] and in the HIV protease database [3]).

The position, frequency, temperature factor and bonding distances of a given hydration site can be analyzed statistically and then discussed from the point of typical solvation patterns corresponding to a given protein surface or a specific protein.

Synchrotron x-ray measurements of the HIV protease – inhibitor complexes at low temperatures (100 K) enable an extended analysis of localized solvent. 301 water molecules have been localized in one of these complexes (1.8 Å resolution). A detailed analysis yields 30 continuous clusters of water molecules internall connected by hydrogen bonds. Localized solvent together with neighboring protein molecules covers about 80% of the complex surface.

1. P.A. Karplus, C. Faerman, *Curr.Opin.Struct.Biol.*, **4** (1994) 770 - 776.

2. H.M. Berman, J. Westbrook, Z. Feng, G. Gilliland, T.N. Bhat, H. Weissig, I.N. Shindyalov, P.E. Bourne, *Nucleic Acids Res.,* **28** (2000) 235-242.

3. http://www.ncifcrf.gov/HIVdb/.

TERTIARY STRUCTURES OF COMPLEXES AS A BASE FOR PROTEIN –PROTEIN RECOGNITION STUDY

Ľ. Urbánikova, R. Dvorský and J. Ševčík

Institute of Molecular Biology, Slovak Academy of Sciences, 84251 Bratislava, Slovak Republic

Proteins belong to the most important matter in living organisms. Their three-dimensional structure uniquely defines their properties. Every property that characterises a living organism is affected by proteins. Proteins are responsible for enzymatic catalysis, immunity, transport of variety of particles, for senses as sight, hearing etc., they are the crucial components of muscles where they convert chemical energy into mechanical, they have regulatory, structural and other functions in the cells. Performing all of these functions they specifically interact with other molecules. It is why the study of protein – protein recognition is required for understanding the mechanism of many important biological processes and is inevitable for practical applications as for example drug-design.

Microbial ribonucleases and their specific inhibitors are well characterised small and relatively stable molecules consisting of about 100 amino-acid residues. They were cloned, over-expressed and large quantities of highly purified proteins were prepared. Ribonucleases interact with their inhibitors very strongly. Tight binding of the two molecules forming the complex makes it possible to crystallize them and to solve their 3D structure.

Barstar, the specific inhibitor of a ribonuclease isolated from *Bacillus amyloliquefaciens* surprisingly inhibits also ribonucleases Sa, Sa2 and Sa3 isolated from various strains

of *Streptomyces aureofaciens.* The dissociation constant of the complexes of Sa ribonucleases with barstar are in the range from 10^{-10} to 10^{-12} M, while the one of the cognate complex barnase/barstar is 10^{-14} M [1]. The structures of Sa [2], Sa2, Sa3 ribonucleases [unpublished results] and the structure of the complex of RNase Sa with barstar [3] were solved at high resolution.

In spite of the fact that the structure of RNase St from *Streptomyces erythreus* [3]is very similar to the structure of RNase Sa its inhibition by barstar is low ($K_D > 10^{-9}$ M). The structure of the Sa/barstar complex [4] and those of barnase/barstar [5,6] allowed a detailed analysis of interfaces and all intermolecular contacts (electrostatic interactions, hydrogen bonds, van der Waals contacts, hydrophobic interactions) contributing to stability of the complex. Complexes of Sa2, Sa3 and St with barstar were modelled and their energy was minimised using CHARMm [7]. Interfaces were analysed, however, it was not possible to explain satisfactorily low inhibition of RNase St by barstar. Therefore, solvent accessible areas of enzymes and inhibitor molecules and distribution of surface charges were analysed and association free energy and contribution of each individual amino-acid to binding energy of complexes was calculated. Based on this calculation several negatively charged St amino-acids residues, far from the interface, were identified. These amino-acid residues are present neither in barnase nor in Sa, Sa2 and Sa3 ribonucleases. In the model these amino-acids were replaced by alanines (non-polar amino-acid) resulted in improvement of calculated interaction energy. As a result we proposed that these amino-acids (their negative charges) are responsible for weakening the long range attractive forces. Mutants of RNase St are being prepared. Measurement of dissociation constants of the mutants with barstar will verify the hypothesis.

1. Hartley R.W., Both V., Hebert E.J., Homérová D., Jucovič M., Nazarov V., Rybajlák I., Ševčík J., *Protein and Peptide Lett.* **4** (1996) 225-231.

2. Ševčík J., Dauter Z., Lamzin V.S., Wilson K.S., *Acta Cryst. D***52** (1996) 327-344.

3. Nakamura K.T., Iwahashi K., Yamamoto Y., Iitaka Y., Yoshida N., Mitsui Y., *Nature* **299** (1982) 564-566.

4. Ševčík J., Urbániková Ľ., Dauter Z., Wilson K.S., *Acta Cryst D***54** (1998) 954-963.

5. Guillet V., Lapthorn A., Hartley R.W., Mauguen Y., *Structure* **1** (1993) 165-177.

6. Buckle A.M., Schreiber G., Fersht A.R., *Biochemistry* **33** (1994) 8878-8889.

7. Brooks B.R., Bruccoleri R.E., Olafson B.D., States D.J., Swaminathan S., Karplus M., *J. Comput. Chem.* **4** (1983) 187–217.

CRYSTALLIZATION EXPERIMENTS ON THE PLANT PHOTOSYSTEM II REACTION CENTER

I. Kutá-Smatanová[1, 2], M. Šáchová[3] and F. Vácha[1, 3]

[1]*Photosynthesis Research Center, University of South Bohemia České Budějovice, Branišovská 31, 370 05 České Budějovice, Czech Republic*

[2] *Laboratory of Biomembranes, Faculty of Biological Sciences, University of South Bohemia České Budějovice, Branišovská 31, 370 05 České Budějovice, Czech Republic*

[3] *Institute of Plant Molecular Biology, Academy of Sciences of the Czech Republic, Branišovská 31, 370 05 České Budějovice, Czech Republic*

Photosystem II is a large pigment-protein complex located in the photosynthetic membrane of green plants, algae and cyanobacteria. It is responsible for the photochemical splitting of water into protons, electrons and molecular oxygen by utilizing sunlight. For its central role in bioenergetics, photosystem II has been the subject of many crystallization attempts [1,2,3].

The complex of photosystem II of higher plants consists of the reaction center proteins D1 and D2 plus α- and β-subunits of cytochrome b-559, two chlorophyll-binding internal antenna proteins CP43 and CP47 and the complex of manganese-stabilizing proteins of 33, 23, 16 kDa. While the reaction centers and the internal antennae are formed by membrane proteins, the manganese-stabilizing complex consists of membrane extrinsic proteins.
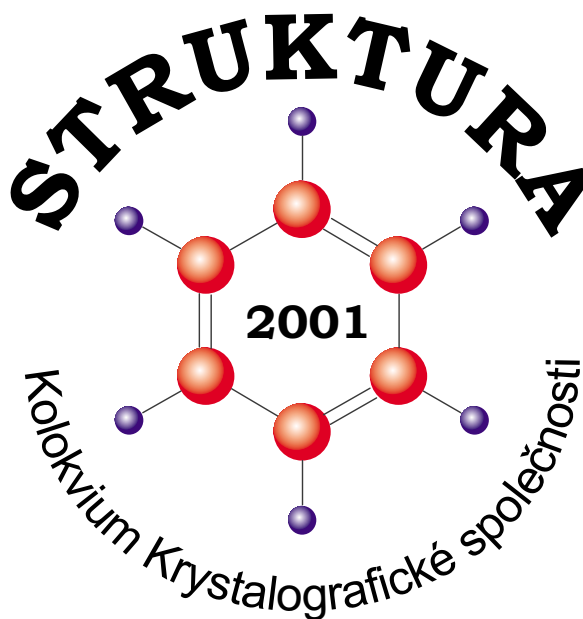
For our experiments we have used the five-chlorophyll reaction center of photosystem II. This five-chlorophyll reaction center of photosystem II was isolated from pea (*Pisum sativum*) and purified according to Vácha [4]. Crystallization trials have been performed in "Cryschem" plates for sitting drops and in capillary tubes at 277K or 289K. 15-mg/ml (1.3 mg/ml chlorophyll *a*) protein has been mixed with different type of detergents and additives used in the crystallization experiments. We have either used the commercial solutions for membrane protein screening "MembFac" of Hampton Research or solutions exactly prepared by us. 50 commercial solutions and 50 different kind of detergents have been available for experiments. According to the adventitious information about a crystallization of photosynthetic reaction centers we have used solutions containing PEG as precipitant. Concerning detergents we have proceeded in accordance with literature data and up to this day we have tried 15 different detergents, detergents with different alkyl chain length and mixtures of detergent. Processes inside the drops have been observed during the period of 2-4 weeks at 289K and 4-6 weeks at 277K. The major part of drops contained precipitates, separated phases or segregated carotenoids in various forms. We have already found for crystallization experiments acceptable pH rate around 7.00 ($\pm$ 0.50), the precipitant PEG4000 or PEG6000 (in the case of using a commercial solutions without PEGs, we have observed the clear drops without precipitate or other formations). For

detergents, at the present of 1-heptyl-β-D-glucosid and 1-octyl-β-D-glucosid, 1-nonyl-β-D-glucosid and their thio forms such as heptyl-β-D-thioglucosid and 1-octyl-β-D-thioglucosid, carotenoids are separated from the protein samples. Nowadays crystallization experiments are still in the progress; we have tried to use new kind of detergents and their mixtures and new crystallization conditions as well.

1. Adir N. "Crystallization of the oxygen-evolving reaction centre of photosysytem II in nine different detergent mixtures", *Acta Cryst*, **D55** (1999) 891-894.

2. Kuhl H., Kruip J., Seidler A., Krieger-Liszkay A., Bünker M., Bald D., Scheidig A.J., Rögner M. "Towards Structural Determination of the Water-splitting Enzyme", *J. Biol. Chem*., **275** (2000) 20652-20659.

3. Zouni A., Witt H-T., Kern J., Fromme P., Krauss N., Saenger W. and Orth P. "Crystal Structure of Photosystem II from *Synechococcus elongatus* at 3.8 Ĺ Resolution", *Nature* **409** (2001) 739-743.

4. Vácha F., Joseph D.M., Durrant J.R., Telfer A., Klug D.R., Porter G., Barber J. "Photochemistry and spectroscopy of five-chlorophyll reaction center of photosystem II isolated by using a Cu affinity column", *Proc. Natl. Acad. Sci. USA*, **92** (1995) 2929-2933.

18. - 22. 6. 2001